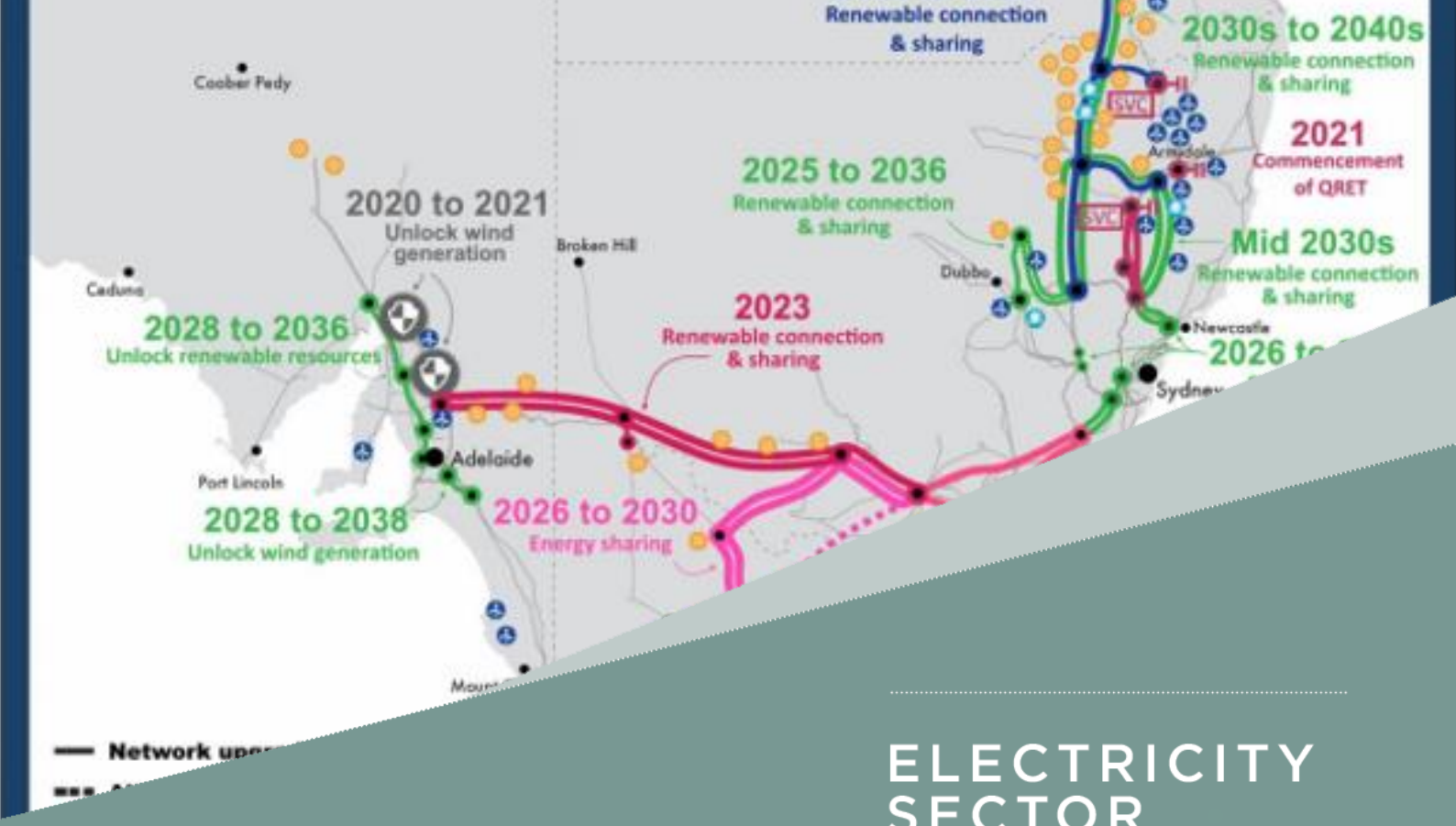

ELECTRICITY SECTOR CLIMATE INFORMATION PROJECT

ESCI Technical Report

Downscaling and evaluating data sets

June 2021

Australian Government
Department of Industry, Science, Energy and Resources

CSIRO

AEMO
AUSTRALIAN ENERGY MARKET OPERATOR

Australian Government
Bureau of Meteorology

Contents

Summary ..... **ii**

1. Objectives of downscaling **4**

2. ESCI downscaling experiment design **5**

2.1 Delta-scaling 6
2.2 Quantile Matching for Extremes 6
2.3 BARPA v1.2 7
2.4 NARCliM v1.5 8
2.5 CCAM v1911 9

3. Data products from ESCI downscaling **10**

3.1 Point location datasets 10
3.2 Regional average datasets 11
3.3 Time-averaged national gridded datasets 12
3.4 Calibrated datasets using QME 12
3.5 Climate extremes datasets 12
3.6 Raw datasets 13

4. Model evaluation **13**

4.1 Current climate: model evaluation 13
4.2 Current climate: representation of extremes 17
4.3 Current climate: model anomalies correlated with NINO34 22
4.4 Current climate: Comparison of fields for summer 27
4.5 Projected change: representing the range of possibilities from CMIP5 models 32
4.6 Projected changes: Realised added value 38

5. Conclusions **47**

6. References **50**

Acknowledgement:

The Electricity Sector Climate Information (ESCI) was a collaboration between CSIRO, the Bureau of Meteorology and the Australian Energy Market Operator. The Department of Industry, Science, Energy and Resources provided funding for the project.

Summary

This report provides information regarding the ESCI downscaled regional climate model (RCM) projections for Australia. The aim is to produce weather and climate data with finer spatial and temporal resolution than global climate models (GCMs) for enhanced climate change projections information. In particular, the ESCI downscaling data are intended to contribute to an enhanced representation of plausible future projections, including of extreme events, relevant to energy sector applications such as future planning around reliability and resilience (e.g., hazard-specific case studies and risk assessments). We describe the approaches used to create the downscaled climate datasets, drawing on various methods for downscaling as applied to a range of GCMs under different emission pathways. Post-processing of the downscaling projection data is also described, including calibration based on assessments and evaluations using observations-based data. We also explain some of the analysis for quantifying Realised Added Value and calculating average recurrence intervals for 1-in-5 year, 1-in-10 year and 1-in-20 year events.

The model evaluation results indicate that downscaling can play an important role in providing a more comprehensive representation of plausible future projected changes, particularly in relation to regional details for hazards and extremes. We also note the creation of some hazard datasets (e.g., to support bushfires, extreme temperatures and winds), with those details provided in the ESCI Standardised Method for Projections Likelihood (SMPL) report.

Key findings from this report are:

- The ESCI project delivered a large step up in regional climate modelling for Australia, including the first production of BARPA (Bureau of Meteorology Atmospheric high-resolution Regional Projections for Australia) projections for user applications, as well as new CCAM (Conformal Cubic Atmospheric Model) projections. It also included the new NARCliM (NSW and ACT Regional Climate Modelling) projections, based on CMIP5 GCMs. A calibration method was also applied to the regional climate projections, with that method having special attention to extremes (based on quantile matching). This was the first time that such a method was used for regional projections in Australia, further helping to improve the data for user applications as compared to what was previously available
- Regional models are found to add 'Realised Added Value' with respect to the host GCM in general and for extremes, as well as in areas of complex topography near coastlines (noting that this is where a lot of Australia's population and infrastructure are located).
- Regional models are found to perform with biases that can be comparable in size to the biases found in the host GCMs, such that appropriate calibration methods are recommended (as applied for the project outputs as detailed in this report).
- Realised Added Value can be further improved by applying bias correction methods, with better results than if the host GCM is bias corrected, as another demonstration of the value of downscaling.
- The set of regional model projections available for Australia has improved significantly through this project, providing additional diversity of approaches and enhancements for existing approaches. The set of RCM projections are somewhat representative of the range of projected change from the broader set of GCM projections. However, the smaller number of regional climate model experiments compared to CMIP global models, means that GCM projections data may also be useful lines of evidence to consider depending on the application. Production of some calibrated GCM projections are also described in this report, to further broaden the range of available projections information provided through this project.

- The regional climate simulations appear to be producing plausible projections (e.g., with respect to climate drivers such as the El Niño – Southern Oscillation). Future analysis may also provide more insight on the downscaling projections, as well as future activities that may increase the set of downscaled regional projections available in the future.

It can be time-consuming and complex to deal with data from many different models, and there was a clear message from the electricity sector that they wanted guidance on a minimum set of data that could be used for risk assessment. The recommendation of the ESCI project was informed by the analysis described here and is provided in a separate document: ESCI Key Concept – ESCI recommended data sets, testing and validation. The recommendation considered the strengths and weaknesses of the datasets described above and the range of projected climate change in each, The project then recommended a subset of four models that sample key uncertainties and can be used in most risk assessments[13]. The minimum recommended datasets are listed in Table 1 below.

Table1: ESCI project recommended data sets. ESCI Guidance notes that best and worst cases are context-specific to the application and can be different for different regions of Australia. This default considers temperature and rainfall for most regions of Australia. Different downscaling and post-processing techniques give different results: other choices should be considered in addition wherever possible

	Global Climate Model	Downscaling model	Northern Australia	Southern Australia	Eastern Australia	Inland (Rangelands)
1	GFDL-ESM2M	CCAM	Warm Dry	Warm Dry	Warm Dry	Hot Dry
2	CanESM2	NARCliM-j	Hot	Warm	Hot	Hot
3	ACCESS1.0	BARPA	Mid case	Mid case	Mid case	Mid case
4	NorESM1-M	CCAM	Warm Wet	Mid case	Warm Wet	Warm Wet

1. Objectives of downscaling

In order to enhance the existing climate projection datasets available for Australia, we have developed additional downscaling datasets and collaborated to include NARCliM regional projections (in particular noting the NSW DPIE as a key agency for supporting NARCliM usage here for the ESCI project). These downscaling datasets differ from their parent GCMs in several ways, including:

- Finer spatial and temporal resolution of the projection data
- Improved representation of some extreme weather events
- Additional variables relevant for the electricity sector that are not available in the CMIP5 GCM datasets
- Improved representation of coastal and urban regions as well as areas of complex topography
- Finer spatial representation of land cover characteristics.

During the ESCI project, downscaled datasets have been made available in case studies and for stakeholders to aid with assessing risk of different hazards under future global warming pathways. Examples include:

- Extreme temperatures
- Bushfires
- Hydrological projections

These hazard datasets are described and analysed in the Standardised Method for Projections Likelihood (SMPL) report that considers multiple lines of evidence (e.g., observations and physical process understanding) in addition to the projection data detailed in this downscaling projections report. Details on downscaling applications during the project are also contained in the case study report for individual hazards, which involved user co-design and guidance on what information and data needs are most useful for their applications. Such user engagement examples during the project helped guide the downscaling and postprocessing that was done to lead to the end products for the projections as described in subsequent sections of this report.

This report describes the downscaling work undertaken for ESCI, and documents model evaluation and calibration for resultant data products. The report also addresses the following points pertaining to the ESCI downscaled datasets:

- What is the methodology behind the downscaling used for each dataset?
- What evaluation and calibration were applied to help them be more fit for purpose?
- What data products are available for stakeholders and researchers?

The report also provides additional analysis on downscaling performance under the appendix for specific models.

Note that the purpose of the ESCI downscaled datasets is to supplement and enhance the available climate projection data (such as that available on Climate Change in Australia (CCiA)), so that the electricity sector can make better-informed decisions to manage climate risk. These datasets are not intended to replace existing analysis based on GCMs nor invalidate any previous analysis. Rather we

envisage that these datasets will be useful for stakeholders and researchers who have already employed some level of analysis of climate projections (e.g., based on CCiA), but need additional information, additional resolution, additional variables or more nuanced calibration applied (e.g., for representing extremes in 'user-ready' data).

Finally, it is worth acknowledging that the science of climate projections and global warming is continuing to evolve and improve. New model intercomparison experiments such as CMIP6 will provide additional insights in the future. Also, new regional projections from a range of sources will help to better understand the impacts of the projected changes in climate. Nevertheless, the data presented here is consistent with our present understanding of climate change and should continue to help stakeholders better understand the climate change risks that they may be facing now as well as in years and decades to come.

2. ESCI downscaling experiment design

The experimental design for ESCI regional climate projections is based on a multi-method, multi-model approach, as no single regional modelling approach can claim to be perfect for representing future climate changes. Considering an ensemble of regional climate model (RCM) approaches can therefore help provide improved representation of the range of future climate change. Using a multi-model and multi-method approach is consistent with international best practice (e.g., Christensen et al 2007, Giorgi and Gutowski 2016). The differences in the projections by different downscaling methods can also be valuable for estimating the degree of confidence in the regional projections (combined with the broader uncertainly from the CMIP5 GCMs), where more consistent projections between modelling approaches can generally be treated with higher confidence than for predictions with larger variation between modelling approaches.

For ESCI we considered several approaches to statistical calibration and dynamical downscaling, namely:

- Delta-scaling of historical weather data using projection changes from GCMs – see Climate Change in Australia Technical Report section 9.3.4 (statistical calibration/downscaling)
- Quantile Matching of Extremes (QME) of simulated weather data using quantile adjustments from historical weather data (statistical calibration/downscaling)
- Dynamical downscaling with BARPA (based on the Unified Model)
- Dynamical downscaling with CCAM
- Dynamical downscaling with NARCliM v1.5 (using existing data from the NARCliM CORDEX simulations based on the Weather Research and Forecasting model)

The above list represents a combination of statistical calibration and dynamical downscaling approaches, as well as varying levels of complexity. Although no single approach is universally preferred for all applications, some methods may already be used by some stakeholders of ESCI and it is important to compare these methods to other approaches. Furthermore, we find that combining approaches often leads to better outcomes (e.g., as is the case for QME with regional models as detailed in later sections of this report). In the following sub-sections, we outline the design of each of the individual calibration and downscaling methods.

Table 1 summarises the CMIP5 GCMs downscaled by the various methods described in this report. Seven of the eight CMIP5 GCMs were recommended in Box 9.2 of the Climate Change in Australia Technical Report[1]. Note that different techniques have been applied based on different GCMs in some cases, with the GCM ACCESS1-0 used by all methods and hence is a useful point of comparison across the different techniques.

Method	ACCESS 1-0	ACCESS 1-3	CanESM2	CESM-CM5	CNRM-CM5	GFDL-ESM2M	HadGEM2-CC	MIROC5	NorESM1-M	Spatial	Temporal	Time period	Emission pathway
CMIP5 GCM	■	■	■	■	■	■	■	■	■	200km	daily	2020-2039, 2040-2059, 2060-2079, 2080-2099	2.6, 4.5 and 8.5
Delta-Scaling	■		■	■		■	■	■	■	5km	30min	1980-2060	4.5 and 8.5
QME	■				■	■		■		5km	daily	1950-2099	4.5 and 8.5
BARPA	■									12km	30min	1980-2099	8.5
NARCliM v1.5	■	■	■							50km	1hour	1950-2100	4.5 and 8.5
CCAM	■		■			■		■	■	12km	30min	1980-2099	4.5 and 8.5

Table 1: Summary of statistical approaches and dynamical downscaling methods and their host GCMs for ESCI. CCAM only downscaled RCP8.5 for CNRM-CM5.

2.1 Delta-scaling

Delta-scaling is a technique where the monthly-mean change predicted by a GCM is applied to a high-resolution historical weather dataset (e.g., on a 5km x 5km grid). This approach is cost effective for producing a high-resolution dataset and only requires monthly-mean changes from a GCM, making a wider range of climate change scenarios more accessible. The method does assume that all parts of the probability distribution change by the same amount (i.e., the mean and the extremes) and that the sequencing of events in the future will be the same as the past. While these assumptions are broken in many cases it is nevertheless a useful first estimate particularly for temperature. For ESCI, this method has been modified to allow sub-daily data to be processed based on daily maximum and minimum temperatures.

2.2 Quantile Matching for Extremes

Climate model simulations approximate daily weather data, but they are not a perfect match to historical data, so their output cannot be used directly in risk assessments in many cases. The calibration method known as Quantile Matching for Extremes (QME) corrects for bias at individual quantiles (i.e., at different parts of the occurrence frequency distribution). In particular, the QME method is characterised

[1] ACCESS1-3 is an additional model that was not part of the CCiA recommended models.

by special attention in relation to the calibration of extreme values. The calibrated weather data retain the characteristics simulated by the climate model, with adjustments based on historical weather data. For further details on the QME method, see Dowdy (2020) with previous examples of its application including for GCMs in relation to fire weather projections (Dowdy et al. 2019).

The QME method has been applied for some key datasets as part of ESCI, including for temperature, rainfall and Forest Fire Danger Index (FFDI, McArthur 1967) based on the output from various GCMs, as well as from various regional climate models (RCMs). The assessment details on these datasets including with QME applied, are provided in subsequent sections.

2.3 BARPA v1.2

Bureau of Meteorology Atmospheric Regional Projections for Australia (BARPA, Su et al. 2021) is developed at the Australian Bureau of Meteorology (BoM) with collaborations with the UK Met Office and other Unified Model partners. It uses the same modelling components deployed in the BoM's short-range and seasonal weather prediction systems (Australian Community Climate and Earth-System Simulator (ACCESS)) and the Australian regional reanalysis (BARRA; Su et al. 2019; Su et al. 2020). BARPA uses a limited-area regional climate model (RCM) configuration of the moderate-resolution global and kilometre-resolution regional models used at BoM and Met Office. These configurations have been tested and used in the Met Office's UK Climate Projections 2018 (UKCP18, Murphy et al. 2018), and are adapted for Australian local conditions.

In BARPA, the moderate-resolution RCM, BARPA-R, is configured with 70 vertical levels and a 12 km horizontal resolution grids over eastern Australia. Reacting to the large-scale forcing by the global models at its domain boundaries (lateral and sea surface) and smaller-scale land characteristics (land sea boundary, land cover, and topography), the BARPA-R model dynamically simulates fine-scale structures based on its own physics. ERA-Interim and CMIP5 ACCESS1-0 (historical and RCP8.5 for future scenarios) are the two driving global models used to complete 1990-2015 and 1960-2099 simulations, respectively.

In these runs, changes in aerosol optical and cloud properties due to radiative forcing are included by prescribing monthly fields of optical properties and cloud droplet number concentration. These fields are generated by combining background aerosol climatology estimated from a pre-industrial forced lower-resolution global atmosphere simulation with a prognostic aerosol scheme, with time-varying anthropogenic aerosol changes from the MACv2-SP (Max Planck Institute Aerosol Climatology v2; Stevens et al. 2016) and stratospheric volcanic forcing.

In addition, a convection-allowing RCM, BARPA-C, was set up to be nested in the BARPA-R ERA-Interim and ACCESS1-0 simulations. This is intended to help provide some insight around potential future changes in extremes, such as for extreme convective wind gusts. This additional downscaling was tested for the warm months during 1986-2005 and 2040-2059 at 4 km resolution in the tropics, and 2 km in the midlatitude.

The ERA-Interim forced BARPA-R simulation has been assessed against observational data for near-surface temperature, vapour pressure and precipitation and BARRA-R regional reanalysis and ERA5 global reanalysis, in a recent paper by Su et al. (2021). BARPA-R reduces biases in ERA-Interim for summertime maximum and minimum temperature and thus is able to reflect more accurate diurnal

temperature ranges. For the winter months, BARPA-R also shows lower bias over the tropics, but for mid-latitude areas, BARPA-R shows biases that are characteristics of BARRA-R. For precipitation, while more capable of simulating more intense rain events than ERA-Interim, BARPA-R and BARRA-R both share the same biases in frequencies of light and heavy rain days during the warm months. These can be attributed to the characteristics of the common underlying model, which will be improved in future development. Nevertheless, BARPA-R can produce a realistic distribution of severe thunderstorm environments as compared with ERA-Interim. It simulated more cyclones than ERA-Interim over the tropics, suggesting a potentially improved ability to represent smaller-scale tropical cyclones.

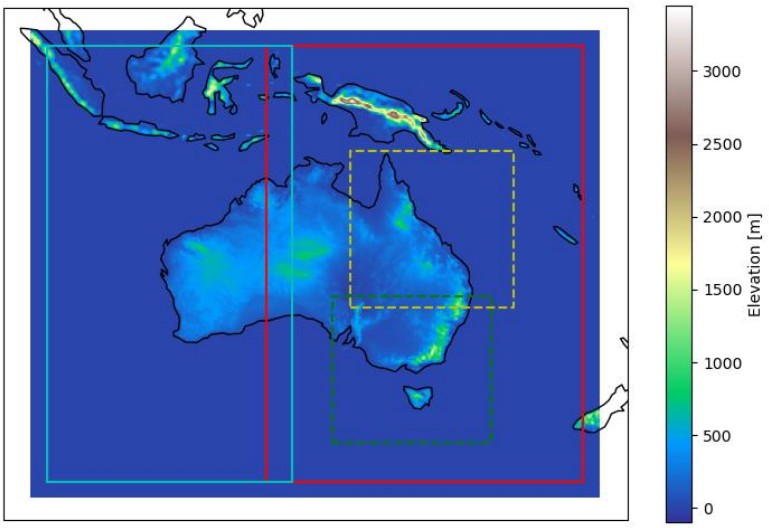

Figure 1: Domains of the BARPA-R RCM model (solid boxes) with the Eastern region shown as the red box and the Western region indicated by the light blue box. Two additional BARPA-C domains are shown in dashed boxes.

2.4 NARCliM v1.5

The NSW/ACT Regional Climate Modelling (NARCliM) project version 1.5 was performed at the University of New South Wales and the NSW Department of Planning, Industry and Environment to extend the NARCliMv1 dataset (Evans et al., 2014). It uses the Weather Research and Forecasting (WRF) modelling system. Within WRF RCMs are formed by choosing the dynamical core and physics parameterisations to use. In NARCliM 36 possible models were tested for their performance and the independence of model errors resulting in two WRF RCMs being chosen for NARCliMv1.5. These RCMs are driven at the lateral boundaries and sea surface by fields from GCMs. For NARCliMv1.5 three GCMs were chosen based on 4 criteria: the GCM performs adequately over Australia; they have independent model errors[2]; they span the future change space for temperature and precipitation in the full GCM ensemble; and they complement the GCMs already used in NARCliMv1. The NARCliMv1.5 simulations have been evaluated along with the broader CORDEX-Australasia ensemble (Evans et al., 2020). The domain that covers all of Australia (CORDEX-Australasia) uses ~50km resolution.

[2] Errors here refers to temperature and precipitation errors across Australia when compared to AWAP.

Simulations were conducted from 1950-2100, for three GCMs under emission pathways RCP4.5 and RCP8.5.

2.5 CCAM v1911

The Conformal Cubic Atmospheric Model (CCAM) (McGregor 2005) is developed by CSIRO Oceans and Atmosphere along with collaborations with University of Queensland, University of Tasmania and overseas contributors. CCAM has a different approach to downscaling compared to the other RCMs described in this report, using a global stretched grid which has finer resolution over a region of interest, but without lateral boundary conditions. Technically CCAM is classified as a global stretched grid model (SGM) rather than a limited area RCM. Nevertheless, for convenience we will continue to use RCM as a general term for the dynamical downscaling models. Since CCAM has no lateral edges, it instead relies on a spectral nudging approach to account for large-scale changes in climate predicted by the host GCM that CCAM is downscaling (Thatcher and McGregor 2009). Basically, this means that CCAM will follow the host GCM for temperatures and winds at large spatial scales (e.g., 3,000km or roughly the size of Australia) above 1.5km above the surface, as well as for surface pressure. However, it is possible for rainfall to be different to the host GCM as, like all dynamical models, CCAM will simulate the rainfall according to its representation of convection and cloud microphysics processes. Surface temperatures over the ocean are interpolated from the host GCM but temperatures over land can change according to the predictions of the CABLE land-surface model included in CCAM.

CCAM used a C288 grid with 35 vertical levels, focused to a resolution of 12km over Australia as shown in Figure 2. The CCAM simulation included a representation of aerosols based on anthropogenic emissions from CMIP5 and natural emission datasets for the sulphur cycle, carbonaceous aerosols, dust and sea-salt. The presence of aerosols can impact radiation and rainfall in the simulation. Simulations were conducted from 1980-2060, with some data extended to 2099, for five GCMs under emission pathways RCP4.5 and RCP8.5.

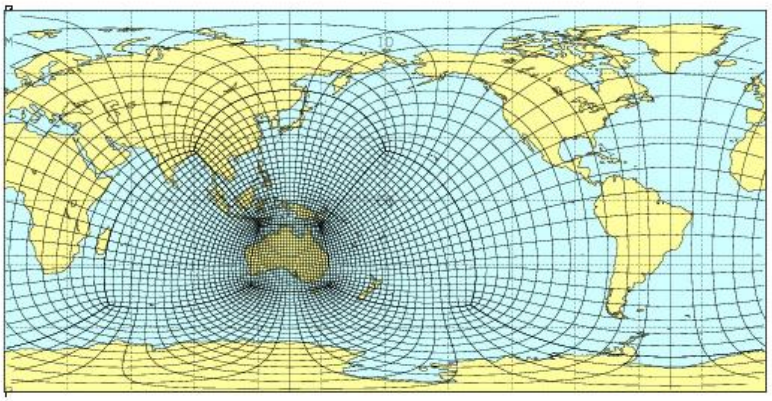

Figure 2: CCAM 12km resolution grid over Australia used for the ESCI project. Note that every 12th grid point is shown in two directions for clarity in the figure.

3. Data products from ESCI downscaling

The ESCI project is providing a number of datasets that are intended to assist the electricity sector with climate change projections. Most climate datasets provide standard climate variables as recommended by CMIP5 for climate studies including daily maximum and minimum temperature, precipitation, surface energy fluxes, windspeed, variables describing solar radiation and clouds, land-surface data such as soil moisture and soil temperature. In addition, we have developed some more specialised datasets which are targeted at the electricity sector. A short description of these datasets developed for ESCI is provided below.

3.1 Point location datasets

An obstacle that prevents stakeholders using the climate projection datasets is the size and volume of the data. This can make it impractical and expensive for users to download. There are multiple strategies to address this problem, with one being the use of point location datasets. These point locations are distributed around Australia to highlight locations of interest for the electricity transmission network. They may represent transmission lines, demand centres, generation sites, and renewable energy sites. These datasets are being made available through the ESCI web page and provide 30 min data for the variables listed in Table 2. A map of the various locations for point data is shown in Figure 3.

Name	Units	Description
Clt	%	Cloud area cover as viewed from the surface
Dni	W m^{-2}	Direct normal irradiance
Ffdi	none	Forest fire danger index (daily only)
Ghi	W m^{-2}	Global horizontal irradiance (also called rsds in CMIP)
Hurs	%	Relative humidity at near surface
Pr	kg m^{-2} s^{-1}	Precipitation
Ps	Pa	Surface pressure
sfcWind	m s^{-1}	Wind speed at 10 m above surface
Tdew	K	Dew point temperature
tdry	K	Dry bulb temperature (also called tas in CMIP)
Wind150	m s^{-1}	Wind speed at 150 m above surface
Wind250	m s^{-1}	Wind speed at 250 m above surface
Winddir	m s^{-1}	Wind direction at 10 m above surface
Winddir150	deg	Wind direction at 150 m above surface
Winddir250	deg	Wind direction at 250 m above surface

Table 2: Description of typical variables available in 30 min intervals for the point locations

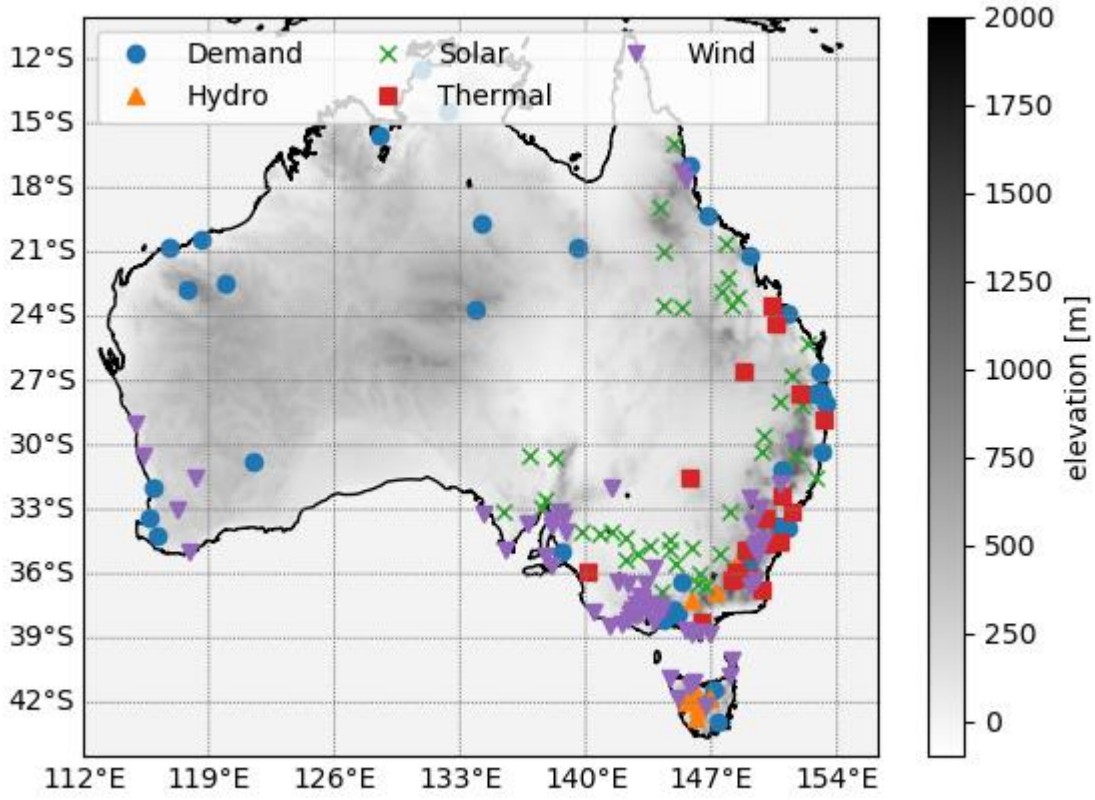

Figure 3: Map of point-location data provided by ESCI. The key indicates the role of each location with a demand center indicated by a blue circle, hydro generation by orange triangles, solar generation by a green cross, thermal generators by a red box and wind generators by a purple triangle.

A second version of daily point location files are based on QME calibrated versions of the GCM and RCM datasets. In this case, calibrated daily data are provided for daily maximum air temperature, daily minimum air temperature, daily precipitation and daily FFDI.

3.2 Regional average datasets

Users of ESCI data may also prefer to use a regional average that is advantageous for capturing more representative changes over the region rather than relying on a single point to represent the changing climate. For ESCI we have produced regional averaged datasets based on the CCiA cluster regions. These datasets are available in 30-min intervals for the same variables shown in Table 2 used for the point locations. As for the point location datasets, daily versions of the regional averaged datasets are also provided for QME-calibrated GCM and RCM datasets.

3.3 Time-averaged national gridded datasets

In cases where users require maps of the climate projection datasets, we have created daily averaged and monthly averaged versions of the data. These datasets vary in spatial resolution from 5km to 50 km resolution depending on the data product. Bias corrected data using QME are available at 5km resolution. Uncorrected data from the BARPA and CCAM downscaled models are available at 12 km resolution. The NARCliM v1.5 downscaling was not funded by ESCI and is available on the CORDEX grid at 50km resolution. Data from each downscaling method are available for the NEM region, with some models also providing national coverage.

3.4 Calibrated datasets using QME

For some applications[3], the presences of climate model biases can undermine the ability to apply climate projections in risk assessments. To this end we have also produced calibrated (i.e., bias corrected) versions of the BARPA, NARCliM and CCAM datasets using the same QME method described in section 2.2 that was applied to calibrate CMIP5 GCMs. Hence the dynamically downscaled datasets all used the same bias correction method when comparing results between the different regional climate projections. This also means that the calibrated GCM and RCM data are all consistent with the observations-based data for the historical period, such as for individual parts of their histograms (i.e., occurrence frequency distributions) including for extremes. Daily maximum 2m air temperature, minimum 2m air temperature and precipitation have been corrected based on AWAP. These datasets are then provided at 5km resolution consistent with the resolution of AWAP.

3.5 Climate extremes datasets

In addition to providing climate projection datasets, the ESCI project has also created a number of derived datasets to provide information about changing climate hazards. To provide information on extreme values from various climate datasets, we have produced Average Recurrence Interval (ARI) data for users. The data were calculated with a Generalised Extreme Value L-moments approach for a series of twenty-year time periods including 1986-2005, 1990-2009, 2000-2019, 2020-2039, 2040-2059, 2060-2079 and 2080-2099. The same approach was also applied to Australian Water Availability Project (AWAP, also known as Australian Gridded Climate Data, AGCD) gridded observed data provided by BoM, to be used to evaluate and benchmark the downscaling performance. Each downscaling dataset for each GCM has been processed independently, allowing users to survey the range of projections or combine the datasets as appropriate. The data is provided for 1-in-2 year, 1-in-5 year, 1-in-10 year and 1-in-20 year return periods for temperature, rainfall and fire weather (using the FFDI), with annual and seasonal datasets. This was also applied for the projections of QME, BARPA, NARCliM v1.5 and CCAM. The ESCI project considered changes in east coast lows (cyclones near midlatitude eastern Australia) following the method described by Murray and Simmonds (1991), and

[3] Applications that have a non-linear response can be particularly susceptible to biases. Examples include modelling crop yields for agriculture, human health impacts and some hydrology applications.

Simmons and Murray (1991) (see also Pepler et al. 2015), while noting this was not a key focus identified by energy sector groups for this project. Extreme wind gusts were a key focus of the project work, and utilised new methods developed in the project as detailed in Brown and Dowdy (2021). Further details regarding the projected changes due to hazards are discussed in the ESCI Standardised Method for Projections Likelihood (SMPL) report.

3.6 Raw datasets

Raw climate projection datasets in up to 30-min intervals and for 50 km to 12 km resolution are available on request. We have assumed that users wishing to source these large datasets have the existing infrastructure and data management skills to download and process such a large dataset. In this case users can contact BoM or CSIRO directly and access the data through an account on the NCI supercomputer, and download the NARCliM1.5 data directly from the Earth System Grid Federation (ESGF) website as part of the CORDEX-Australasia data.

4. Model evaluation

This section examines aspects of the downscaling performance with respect to observations and with respect to the CMIP5 archive of GCMs. In some cases, the model evaluation is focused on Eastern Australia, noting a focus on this region for ESCI (i.e., provided to ESCI stakeholders for the NEM region in eastern Australia).

4.1 Current climate: model evaluation

Evaluation of the current climate simulations is focused on measuring the difference between different downscaling techniques. For many climate projection applications, the variables of interest often include temperature and precipitation, including their biases compared with observations as shown in this section. All biases were calculated for 1986-2005 which is the typical historical reference period for CMIP5 GCMs and are calculated with respect to the AWAP gridded analysis of observations. We have not plotted the biases for QME as they are relatively small compared to the dynamical downscaling biases (i.e., QME application to model data results in a near-perfect match to historical data based on its quantile matching approach, including for extremes), which is a key feature leading to its suitability for producing application-ready data products. Delta-scaling biases are directly related to the host dataset, which is currently based on CCAM.

Figure 4 shows the bias for daily maximum temperature for BARPA, CCAM and NARCliM v1.5 as well as the bias for the host GCMs. In NARCliM v1.5 the J and K model configurations use different physical parameterisations, we have plotted the biases for these two configurations separately. We note that all the models tend to show a cold bias with respect to the AWAP gridded analysis of observations, although the bias does vary with location and between models. Nevertheless, the biases

of the downscaled models are quite consistent in magnitude with the biases associated with GCMs. It is also clear that biases along the Australian alps are broadly similar for the GCMs, but can be reduced significantly by the downscaling approaches. Biases in other regions can increase, such as for an increased cold bias with CCAM in northern Australia.

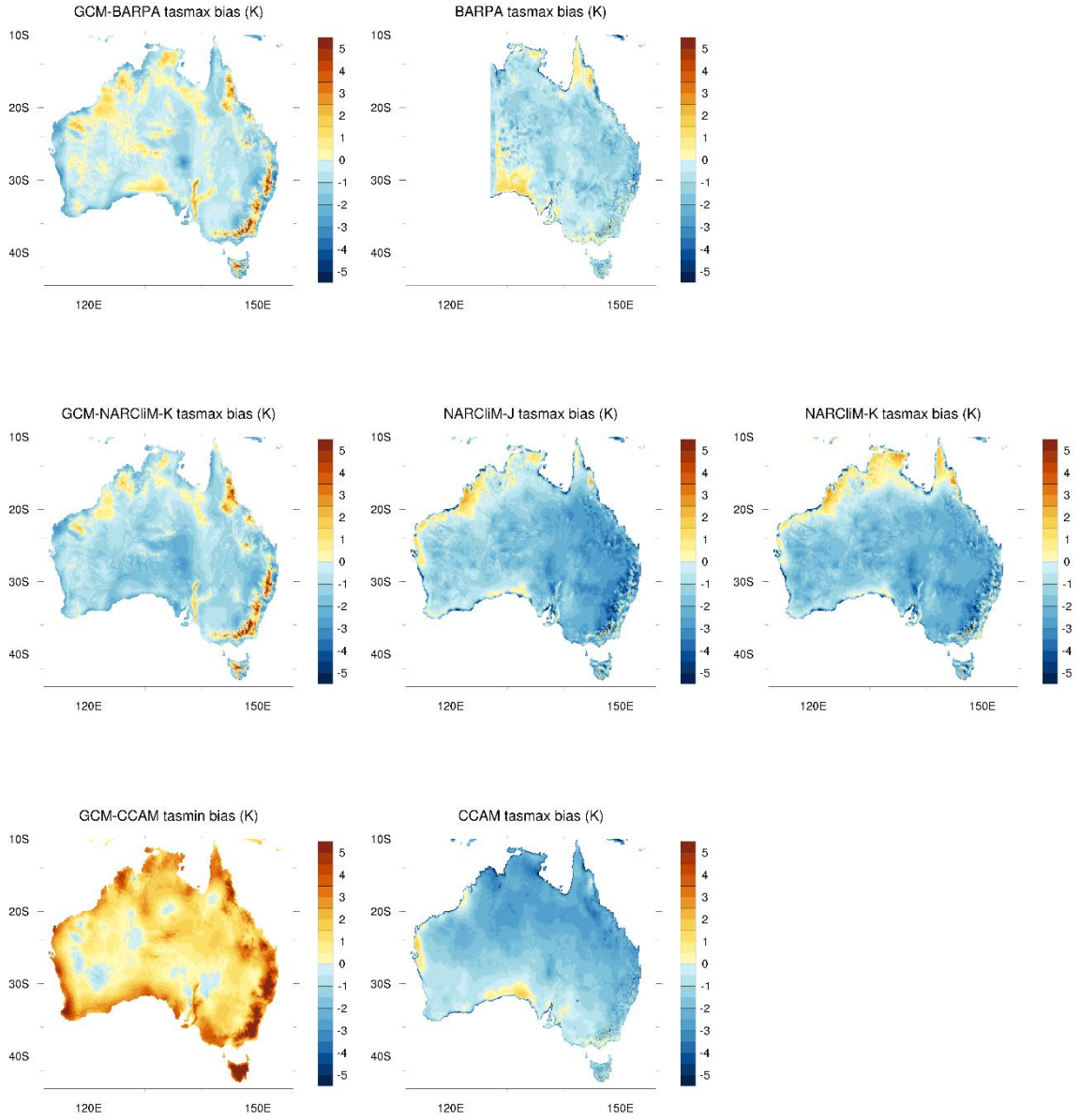

Figure 4: Bias plots for daily maximum 2m air temperature over 1986-2005 between dynamical downscaling models BARPA, NARCliM and CCAM for the top, middle and bottom rows respectively. Left column shows the average bias over the host CMIP5 host GCMs (different GCMs are used for each model as shown in Table 1) whereas the remaining middle and right columns show the RCM performance of the two model configurations in NARCliM v1.5 and a single version of CCAM and BARPA. Biases are calculated with respect to AWAP observed gridded dataset from BoM.

Figure 5 shows the biases for the daily minimum temperature for the dynamically downscaled models compared to the average bias for the host CMIP5 GCMs. Again, biases can vary between location and RCM. However, the strong warm bias in the daily minimum air temperature from the GCMs along the coastlines is much improved in the dynamically downscaled models on average. The cause of the cold

bias in minimum temperature is still being investigated, but is sometimes associated with a reduction in cloud cover or limitations with the land-surface model (i.e., heat stored in the soil).

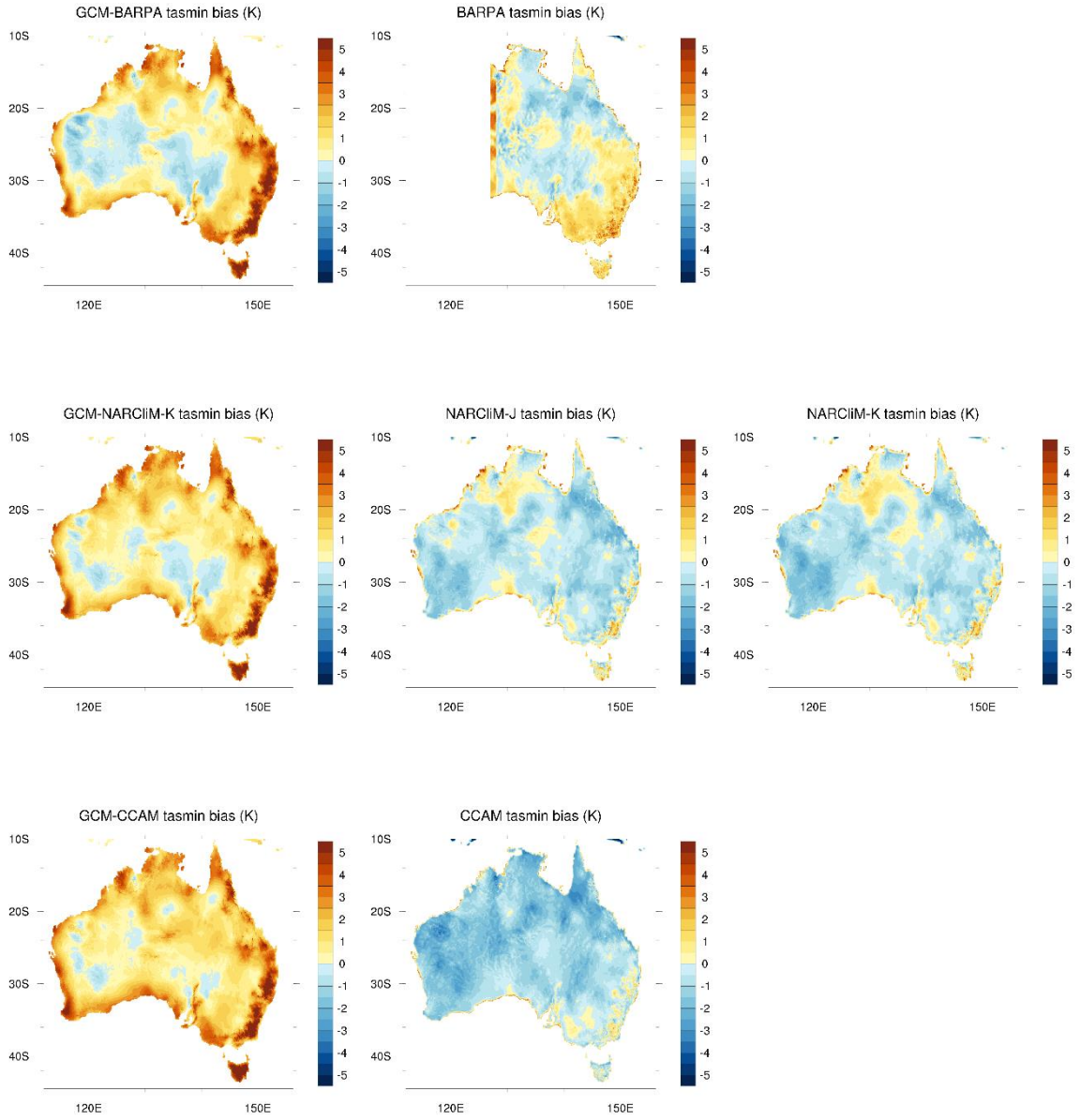

Figure 5: Same as Figure 4, but for daily minimum 2m air temperature with respect to AWAP observed gridded dataset from BoM. The left column is the average results for the host GCMs and the middle and right columns are for the RCMs, including NARCliMs two model configurations. The top, middle and bottom rows correspond to BARPA, NARCliM and CCAM respectively.

Next, we compare the bias in daily precipitation between the host GCMs and the downscaled RCMs as shown in Figure 6. Once more we find that the bias can change between locations and RCMs. Nevertheless, rainfall biases in the GCMs associated with the Australian alps and Tasmania are reduced in general (i.e., regions of complex topography).

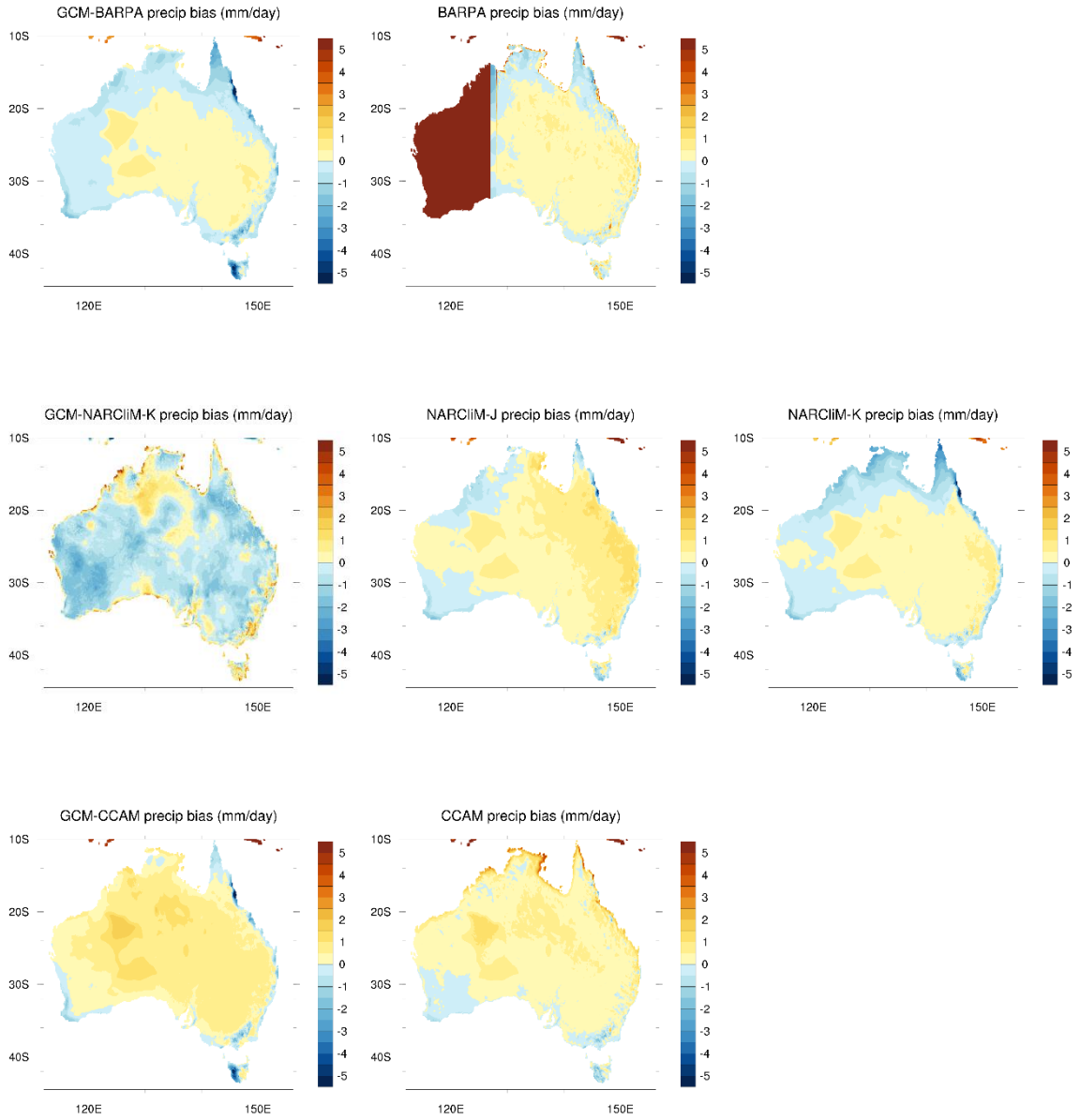

Figure 6: Same as for Figure 4,but showing the bias for daily precipitation with respect to AWAP observed dataset from BoM. The left column is the average results for the host GCMs and the middle and right columns are for the RCMs, including NARCliMs two model configurations. The top, middle and bottom rows correspond to BARPA, NARCliM and CCAM respectively.

Simulation biases can also be broken down by season, although are not shown here in the interests of providing a more succinct summary of the model performance. The downscaling models do change some of the simulation biases, with the most noticeable example being a colder minimum temperature bias, whereas the GCMs typically showed a warm bias. This can be partly due to the choice of downscaling method, but also related to the regional model's land-surface, boundary layer turbulent mixing as well as representation of cloud cover. The RCMs do reduce biases on average when considering areas of complex topography like the Australian alps or Tasmania. It is also expected that precipitation biases may also improve when considering convection-scale simulations (e.g., less than

4km resolution) although these have not been investigated in this study. The issue arises due to the fact that small scale processes (e.g., convection) cannot be explicitly modelled in mesoscale (> about 12km) models such that sub-grid cloud and precipitation are estimated with simplified empirical relations.

4.2 Current climate: representation of extremes

An issue when representing extreme events in climate simulations is having sufficient observations to provide a robust comparison. Insufficient data or inappropriate treatment can lead to 'noisy' and possibly misleading results. To this end we have calculated the Average Recurrence Interval (ARI) for 1-in-5 year, 1-in-10 year and 1-in-20 year events. The results are again compared to AWAP data, although care should be taken when comparing extreme rainfall for gridded data with observations at individual locations as AWAP data may underestimate extremes compared to a point measurement (King et al. 2013).

Figure 7 shows the results from different downscaling methods for 1-in-5 year, 1-in-10 year and 1-in-20 year daily maximum temperature, compared to observations based on AWAP after downscaling ACCESS1-0 across downscaling methods used in ESCI. Note that the NARCliM results are based on 50 km resolution data, the BARPA and CCAM results are based on 12 km resolution data and the observations are based on 5 km data. The models do represent the extreme temperatures to an extent, with 12 km BARPA simulating the hottest temperatures and the 50 km NARCliM results simulating slightly lower temperatures. It should be noted that often the extremes are evaluated at the model native resolution as this is considered a fairer test of what the model can be expected to produce. However, in this case we have evaluated the models with respect to the observed 5 km grid so as to clarify what extremes can be resolved in each dataset (i.e., from the user's perspective).

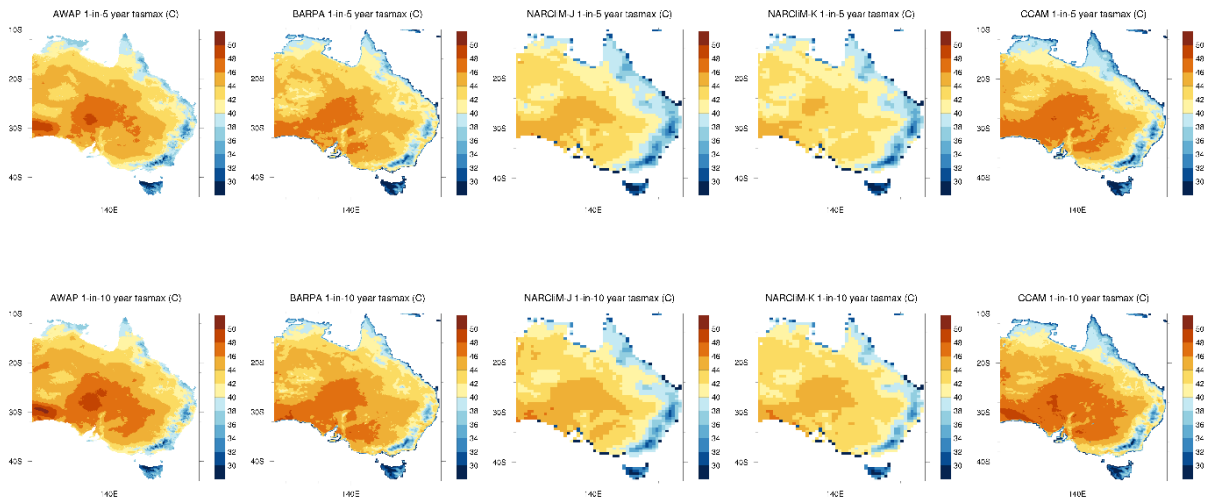

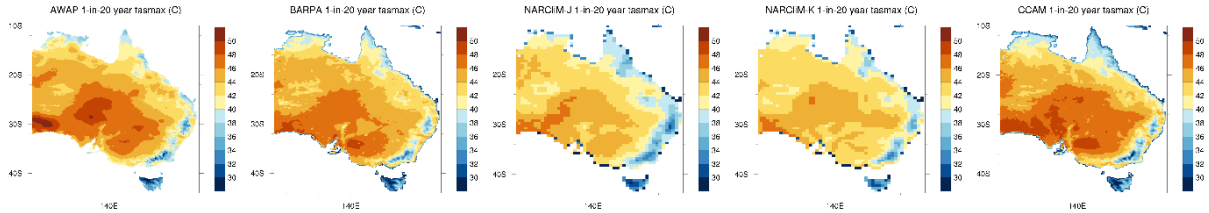

Figure 7: Comparison of 1-in-5 year (top row), 1-in-10 year (middle row) and 1-in-20 year (bottom row) daily maximum temperatures for the different downscaling methods. Observations based on AWAP are shown left column, with BARPA (2nd column), NARCliM J (3rd column), NARCliM K (4th column) and CCAM (5th column). Note that NARCliM simulations are 50 km resolution whereas BARPA and CCAM are 12 km resolution.

Figure 8 also compares the 1-in-5 year, 1-in-10 year and 1-in-20 year extreme daily maximum temperature with respect to the ACCESS1-0 GCM. Comparing ACCESS1-0 GCM in Figure 8 with Figure 7 for the regional models, we note that the regional model improves the representation of extreme temperatures in some regions with respect to the GCM. For example, eastern Australia has a cooler 1-in-20 year temperature in both the AWAP observations and RCM data compared to the GCM datasets. There are also other locations like southern Tasmania where the GCM underestimates the extreme temperatures compared to the regional models.

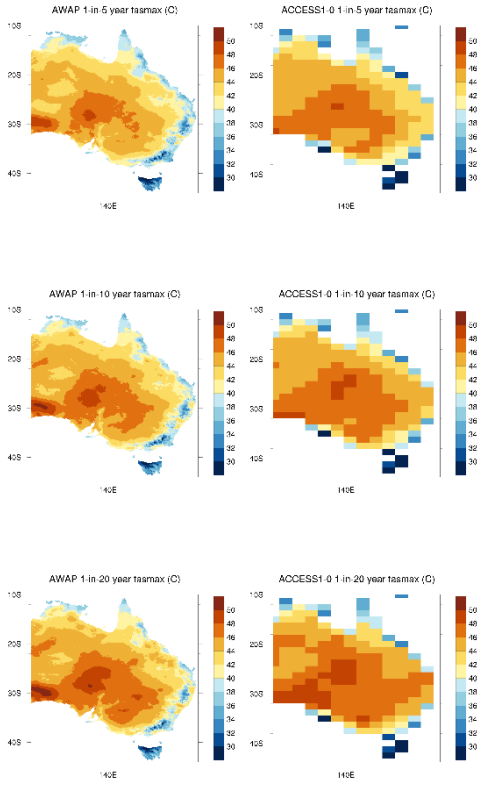

Figure 8: Comparison of 1-in-5 year (top row), 1-in-10 year (middle row) and 1-in20 year (bottom row) daily maximum temperatures with ACCESS1-0 GCM. Observations based on AWAP are shown left column and ACCESS1-0 GCM is the right column. The results can be compared to Figure 7.

Figure 9 describes the ability of the downscaling to represent extreme daily rainfall. The regional models tend to overestimate the extreme rainfall in northern Australia, with NARCliM-K being the lowest. However, the regional models generally perform well over the eastern Australia coastline which has higher extreme rainfall compared to inland.

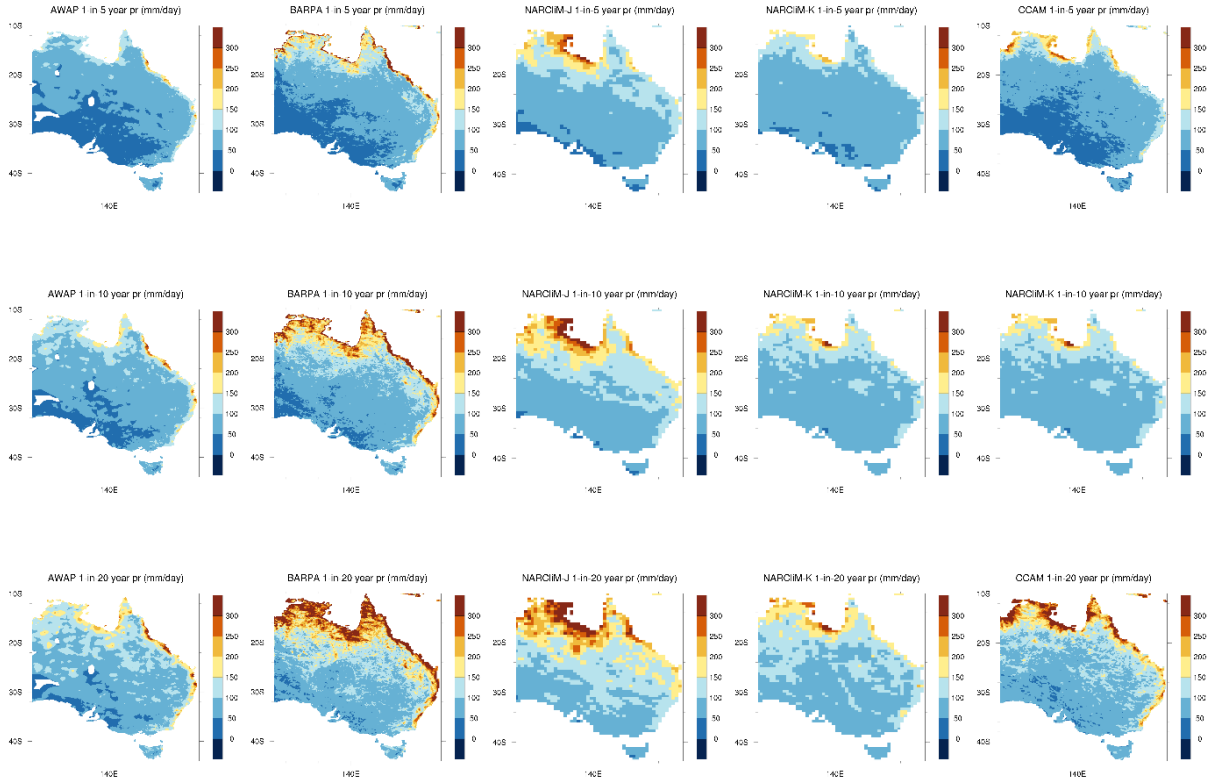

Figure 9: Comparison of 1-in-5 year (top row), 1-in-10 year (middle row) and 1-in-20 year (bottom row) daily precipitation for the different downscaling methods. Observations based on AWAP are shown left column, with BARPA (2nd column), NARCliM J (3rd column), NARCliM K (4th column) and CCAM (5th column). Note that NARCliM simulations are 50 km resolution whereas BARPA and CCAM are 12 km resolution.

We also compare the extreme rainfall from the regional models in Figure 9 with the extreme rainfall simulated by the host GCM in Figure 10. The regional models tend to have a better representation of the extreme rainfall along coastal regions where the GCM underestimates the extreme rainfall (e.g., the eastern Australia coast). There is also a tendency for the ACCESS1-0 GCM to underestimate the extreme rainfall for northern Queensland with 1-in-5 and 1-in-10 year extreme rainfall events, whereas regional models simulate higher extreme rainfall. In some cases, a regional model can overestimate the extreme rainfall in northern Australia with respect to AWAP.

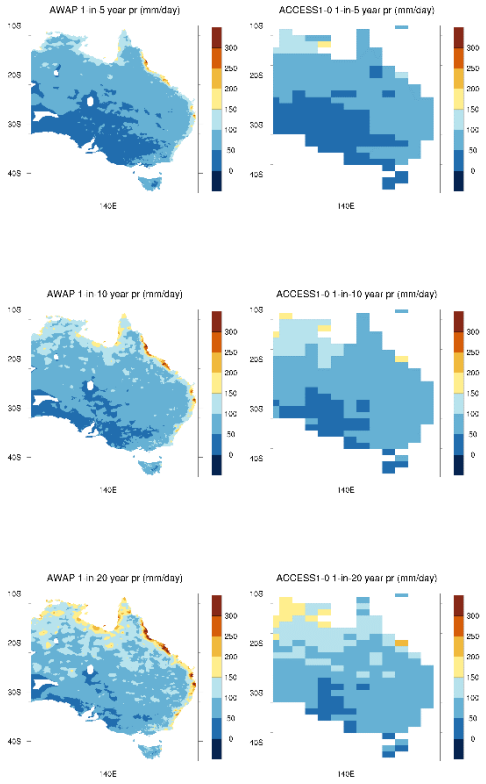

Figure 10: Comparison of 1-in-5 year (top row), 1-in-10 year (middle row) and 1-in-20 year (bottom row) daily precipitation for the ACCESS1-0 GCM. Observations based on AWAP are shown left column and ACCESS1-0 GCM is the right column. The results can be compared to Figure 9.

Although regional models can better represent extremes in various locations, the results are further improved after applying QME calibration. Once QME is applied the extreme temperatures and rainfall are in very close agreement with the AWAP observations. An example is shown in Figures 10 and 11 for BARPA corrected by QME.

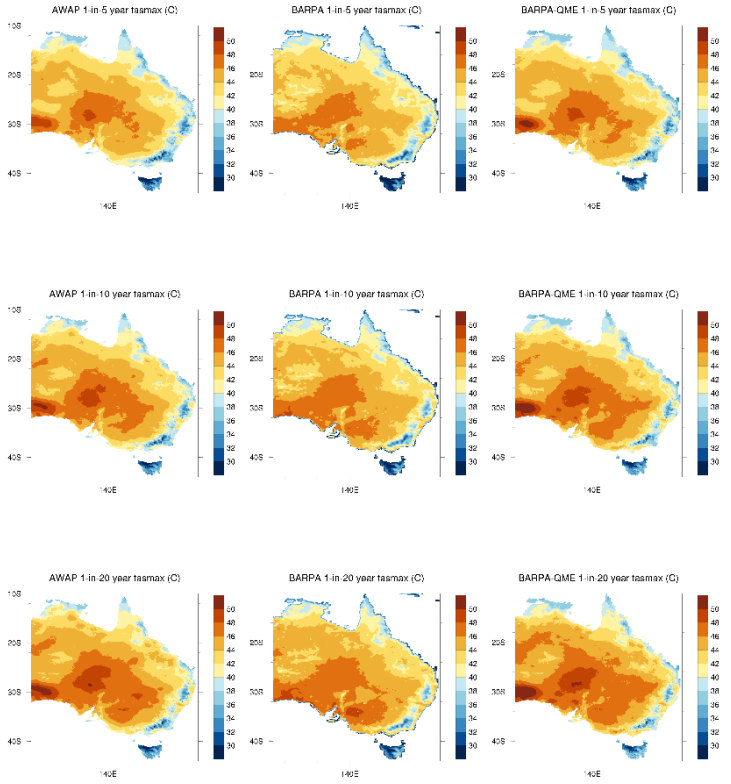

Figure 10: Comparison of 1-in-5 year (top row), 1-in-10 year (middle row) and 1-in-20 year (bottom row) daily maximum temperatures for BARPA after QME has been applied. First column shows AWAP, 2nd column shows uncalibrated BARPA, 3rd column shows calibrated BARPA-QME.

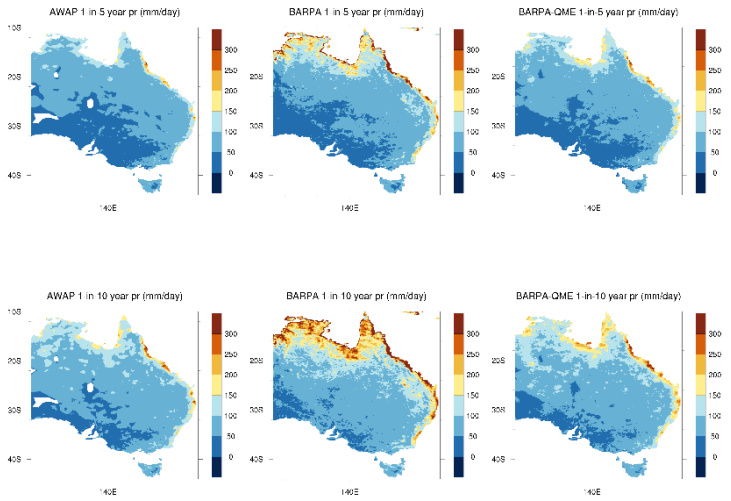

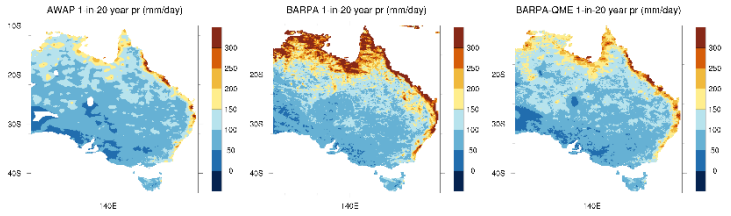

Figure 11: Comparison of 1-in-5 year (top row), 1-in-10 year (middle row) and 1-in-20 year (bottom row) daily precipitation for BARPA after QME has been applied. First column shows AWAP, 2nd column shows uncalibrated BARPA, 3rd column shows calibrated BARPA-QME.

4.3 Current climate: model anomalies correlated with NINO34

A comparison between different regional models BARPA, NARCliM-K and CCAM is shown in Figures 12 to 15, depicting the results of a regression analysis with respect to 2m air temperature and precipitation with respect to the NINO34 index. The CCAM-ACCESS1-0 ACCESS1-0 anomalies in Figures 12 to 15 are broadly similar to those for CMIP5 ACCESS1-0. The CMIP5 models within the six-member ensemble have contrasting NINO34 responses. In particular, the other five downscaled models by CCAM have a drier and warmer response to NINO34 in Sep-Oct-Nov.

The anomalies in both rainfall and daily average 2m air temperature for the QME version of CCAM-ACCESS1-0 are very similar to those for the model output. Note also that daily average temperature is estimated here as the average of daily maximum temperature and daily minimum temperature.

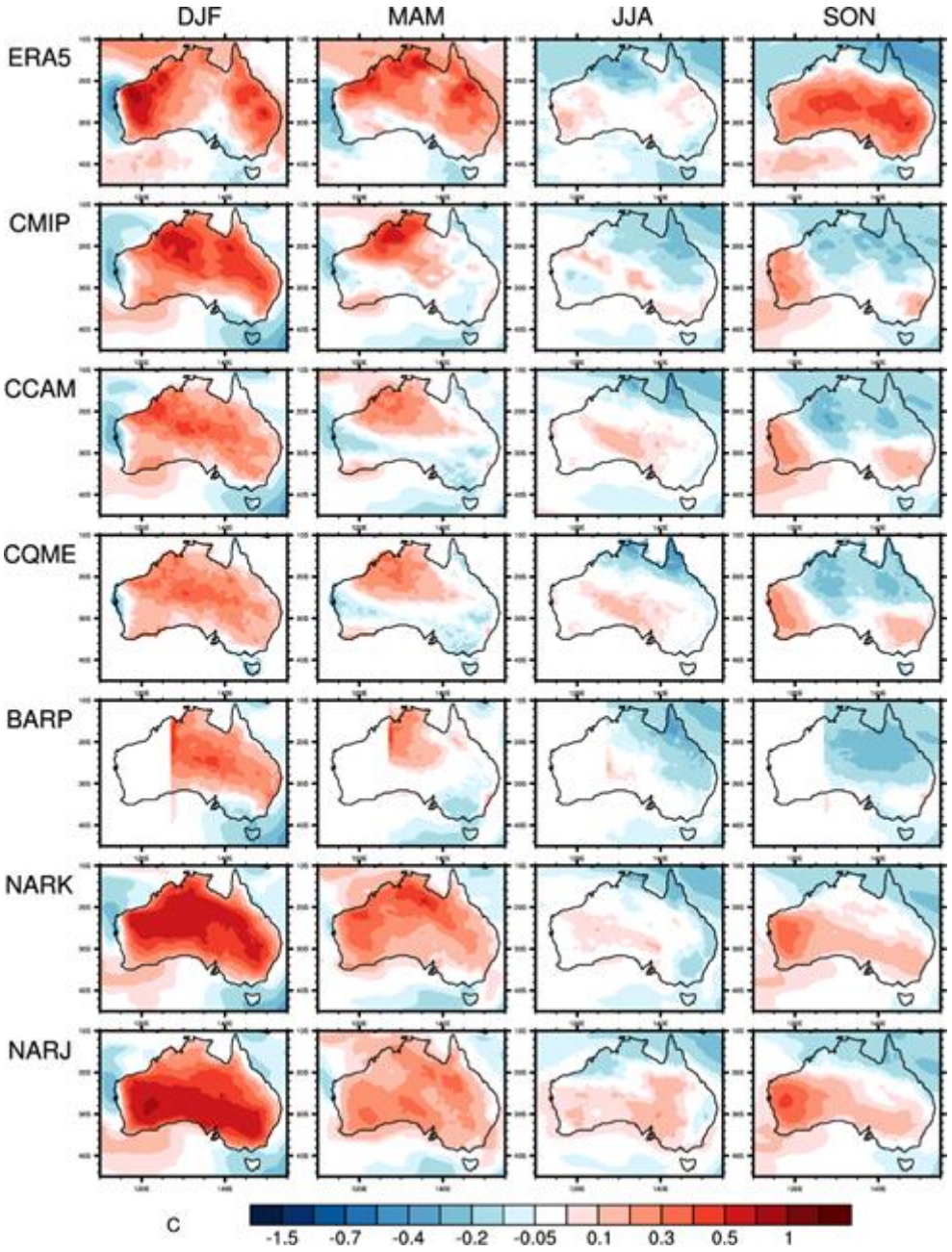

Figure 12: Anomalies of 2m air temperature for a one standard deviation anomaly of the NINO34 index based on regression of seasonal means (as labelled) from years 1980-2019 for five types of data associated with ACCESS1-0: from top to bottom the ERA5 analysis, the CMIP5 model, CCAM, the QME of CCAM, BARPA, NARCliM-K and NARCliM-J. Data off the coast are calculated for CQME but it represents only land (islands). Only every third grid point is used, aside from CMIP5.

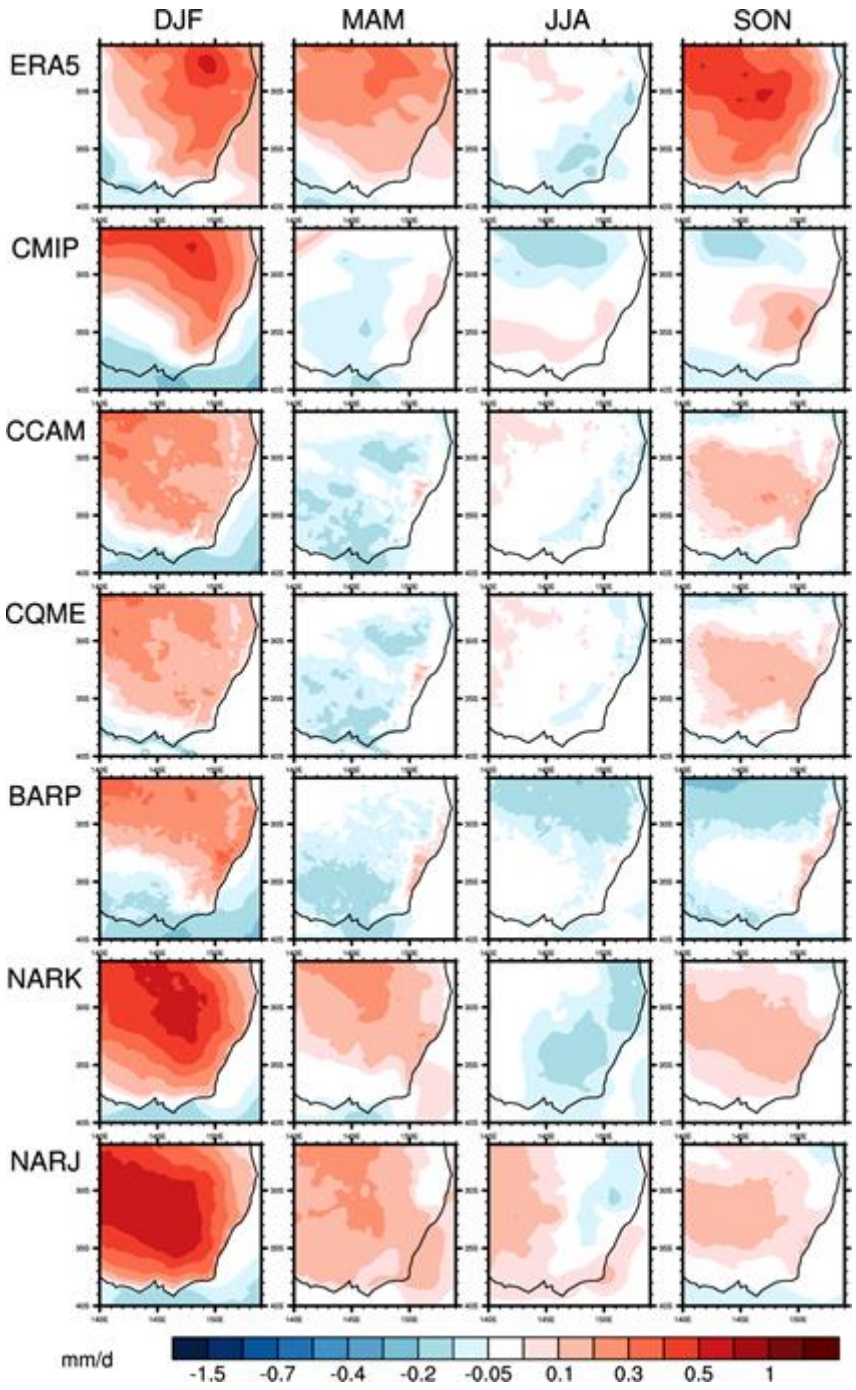

Figure 13: As Figure 12, but for the south east, at full resolution.

The BARPA and NARCliM anomalies are also shown in Figures 12 to 15. From their raw grids, BARPA has more detail than CCAM and NARCliM and this is evident in Figures 13 and 15. NARCliM has been simulated at 50km resolution compared to BARPA and CCAM at 12km resolution. In the case of NARCliM there appears a little less similarity to the ACCESS1-0 results than there is for CCAM or BARPA, which may result from the downscaling technique. For instance, in Mar-Apr-May NARCliM has a mostly drier and warmer south east and interior of Queensland, unlike the other four types. In general, the two NARCliM results appear similar. Some differences could arise by chance, from the sampling of 40 years in the simulation. Further simulations could be used to examine this, and indeed reduce uncertainty in all the results.

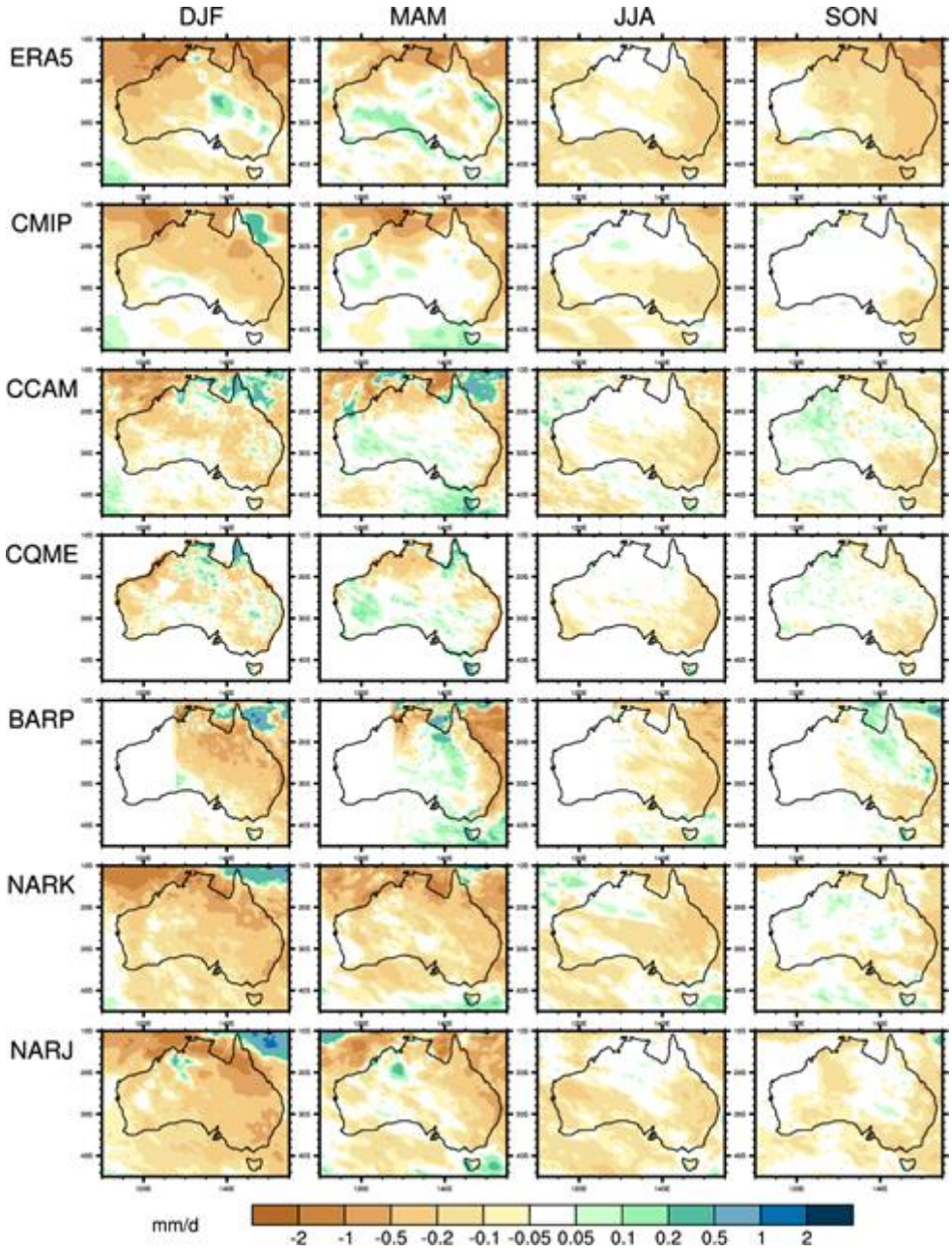

Figure 14: As Figure 12, but for precipitation.

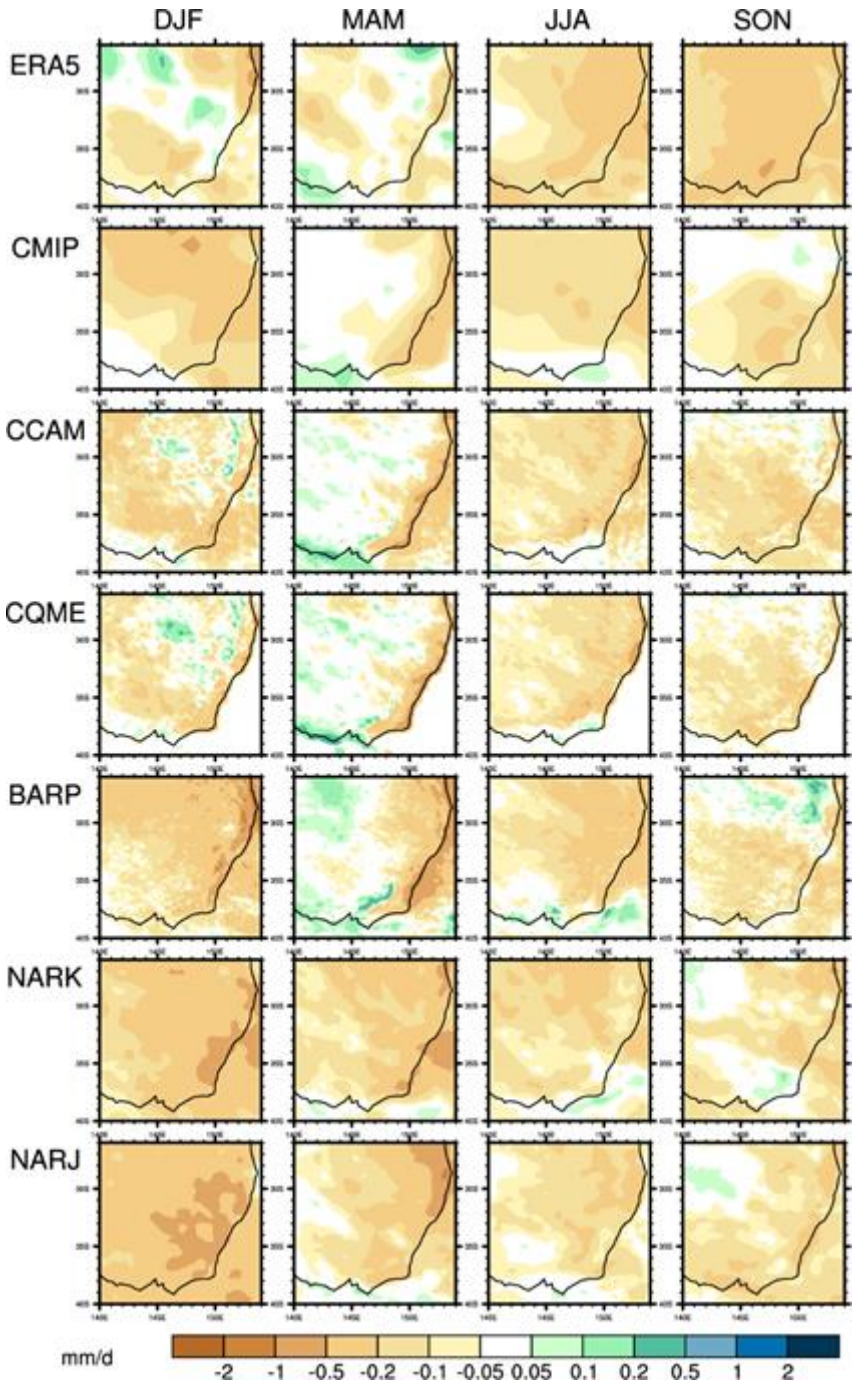

Figure 15: As Figure 14, but for the south east, at full resolution.

The anomalies for sea-level pressure are shown over the Australian domain in Figure 16. The anomalies in sea-level pressure are part of the large-scale circulation changes associated with the ENSO represented in ACCESS1-0. The CCAM anomalies closely match those of the CMIP5 model, probably due to the use of spectral nudging with a 3,000km length scale. The BARPA fields appear not as close, likely because of the lack of constraint on sea-level pressure in the interior of the domain. The NARCliM results are more different, especially in Dec-Jan-Feb. The larger negative rainfall anomalies in

the southeast from NARCliM appear related to the more extensive positive sea-level pressure anomalies.

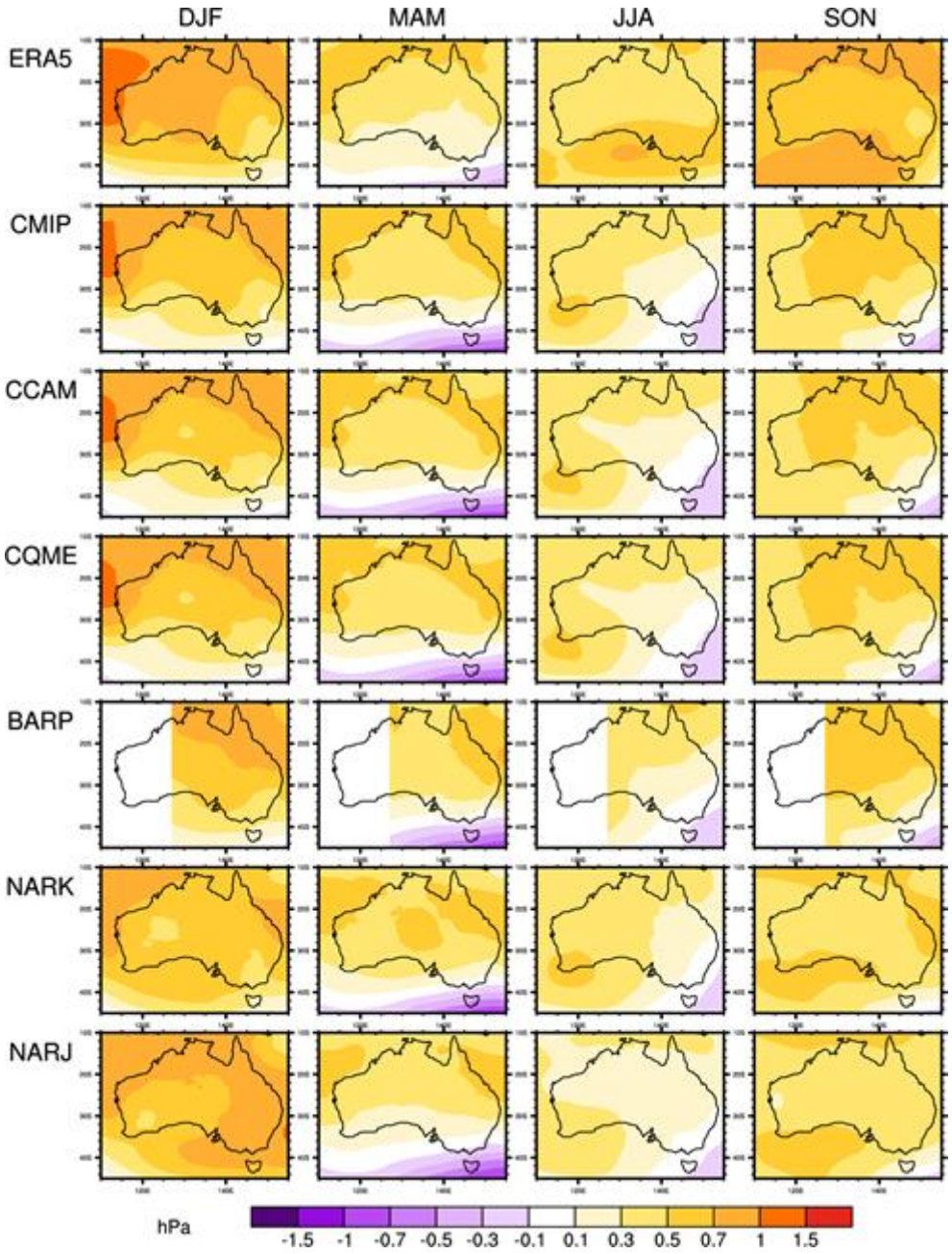

Figure 16. As Figure 12, but for sea-level pressure. Here the CCAM result is used for CQME.

4.4 Current climate: Comparison of fields for summer

Various statistics for the data over eastern Australia are given in Table 3, using ACCESS1-0 as a common host GCM between downscaled models. The eastern Australian region is described in Figure 17, along with sub-regions used later in this section. The spatial mean AWAP summer temperature is slightly higher than from ERA5 (by 0.3°C). This analysis also includes the M score described in

Watterson (2015), which shows the mean-squared error non-dimensionalised by the spatial variance of the field. The M score is useful for providing greater differentiation compared to correlation coefficients in cases where the field has a large spatial variation compared to its mean-squared error. An M score of 0 indicates no skill, whereas an M score of 1000 describes the best possible score. Negative M scores are rare in this context. Table 3 shows that the M score between ERA5 and AWAP is high, and the root-mean-squared difference is low. Removing the spatial mean to form anomaly fields makes a change to the results -indicative of greater similarity. The standard deviation (SD) appears small compared to the mean in each case. However, it is much larger than the bias in the mean of a model, compared to AWAP. The improvement for anomaly fields is higher in cases with larger mean bias. The M score for BARPA is higher than for CCAM, even for the anomaly fields. While still a good score, that for CCAM-ACCESS1-0 is beaten by NARCliM-K-ACCESS1-0. Of course, these runs are downscaling ACCESS1.0, rather than observations. Note that there is a consistency between the rankings of models by M values and root-mean-squared values, as one would expect.

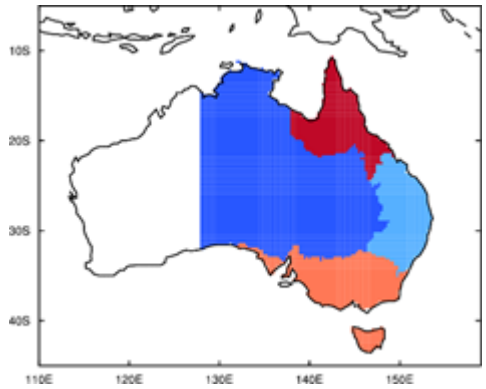

Figure 17. Regions used for summer comparison in this section with red SEN, light blue SEE, orange SES. The combination of all shaded regions indicates the eastern Australia (AUE) region. The data is reduced to a 0.25° grid for plotting.

	AWAP	ERA5	CCAM-ACCESS1-0	NARCliM-K-ACCESS1-0	BARPA-ACCESS1-0
Mean, °C	27.6	27.3	26.6	25.8	27.4
SD, °C	3.64	3.74	3.46	3.34	3.60
M		882	753	639	882
rmse, °C		0.68	1.40	2.08	0.67
anom M		898	829	812	889
anom rmse, °C		0.59	0.95	1.03	0.63

Table 3. Statistics for climatological mean temperature in summer over region Eastern Australia. All fields are interpolated to the 0.25° grid . The statistics are firstly spatial mean and standard deviation (SD), then the M-skill score(M) and root mean square error (rmse), between with the field and AWAP, for the whole field, then for the anomaly field.

The statistics in Table 4 show the results for the climatological mean temperature for summer over Eastern Australia. CCAM has the highest mean of all for ACCESS1-0 downscaling. BARPA-ACCESS1-0 has the lowest mean, with NARCliM-K-ACCESS1-0 in between. BARPA-ACCESS1-0 also has a lower spatial SD, although it is still much larger than the bias in the mean. BARPA-ACCESS1-0 has the lowest M, even for the anomaly. The similarity between ERA5 and AWAP is easily the highest as they are both based on observations.

	AWAP	ERA5	CCAM-ACCESS1-0	NARCliM-K-ACCESS1-0	BARPA-ACCESS1-0
Mean, mm/d	2.81	2.76	3.23	2.73	2.40
SD, mm/d	2.47	2.27	2.17	1.87	1.56
M		876	673	635	601
rmse, mm/d		0.46	1.12	1.19	1.28
anom M		876	694	636	618
Anom, rmse, mm/d		0.46	1.04	1.18	1.22

Table 4. As Table 3, but for mean pr, with units of mm/d.

Since ACCESS1-0 has been downscaled by three models, it is worth giving further details for these cases. Firstly, the downscaled fields are compared with those from ACCESS1-0 itself (both are interpolated to the 0.05° grid). The 4-season average M for each available variable over Eastern Australia is given in Table 5. It is notable that the CCAM sea-level pressure has a high M value; again, this confirms the influence of the driving surface level pressure fields over land. BARPA is very similar to ACCESS1-0 for both sea-level pressure and air temperature, possibly because of the common UM atmospheric formulation. The very different resolutions likely explain the smaller M (larger difference) for precipitation. In general, the three models are providing some similarity in the base climate, but with their own characteristics.

Model	**Air temperature**	**Preciptation**	**Sea-level pressure**	**Average**
CCAM	642	452	879	658
NARK	664	535	599	599
NARJ	658	497	638	598
BARPA	797	491	877	722

Table 5. Scores for region Eastern Australia from both CCAM, NARCliM (NARK,J) and BARPA, showing the similarity to ACCESS1-0. The M scores are averaged over the four seasons, for each variable, then combined.

The corresponding scores showing 'skill' relative to the observed data are given in Table 6. The air temperature score for BARPA-ACCESS1-0 is very impressive. The result for precipitation is only fair, consistent with the above analysis. Interestingly, both the CCAM-ACCESS1-0 and BARPA-ACCESS1-0 values for air temperature and precipitation are higher than in Table 5. Possibly the reduced detail from ACCESS1-0 lowers those air temperature and precipitation scores. The variations in scores across the driver cases seem consistent with those across the CMIP5 models. As an example of bias correction,

the QME version of CCAM-ACCESS1-0 produces climatological fields very close to those of AWAP, with the average M scores close to 1000, although precipitation has some minor deviations. None of the scores indicate a significant problem in any of the data.

CMIP5/ driver	Model	Air temperature	Precipitation	Sea-level pressure	Average
ACCESS1-0	CCAM	742	597	840	726
ACCESS1-0	NARK	746	526	667	646
ACCESS1-0	NARJ	748	595	702	682
ACCESS1-0	BARPA	878	612	749	746
ACCESS1-0	CCAM-QME	990	941		

Table 6. Skill scores for region Eastern Australia from both CCAM and NARCliM (NARK, NARJ). The M scores are averaged over the four seasons, for each variable, then combined.

The overall M score (average for air temperature, precipitation, sea-level pressure) for each region and model is given by the average over the four seasons and three variables, following the method used for CCiA Fig. 5.2.2. The results are given in Table 7 with the regions shown in Figure 17.

CMIP5	AUE	SES	SEE	SEN	Av S,E,N
ACCESS1-0	707	455	452	474	460.3
CanESM2	656	406	407	441	418.0
CNRM-CM5	687	498	393	485	458.7
GFDL-ESM2M	599	268	370	366	334.7
MIROC5	644	353	401	505	419.7
NorESM1-M	601	315	414	369	366.0
AVE	649.0	382.5	406.2	440.0	409.6

CCAM 12km	AUE	SES	SEE	SEN	Av S, E, N
ACCESS1-0	726	670	516	556	580.7
CanESM2	665	569	429	548	515.3
CNRM-CM5	706	657	551	535	581.0
GFDL-ESM2M	616	519	389	404	437.3
MIROC5	658	590	486	495	523.7
NorESM1-M	715	613	563	522	566.0
AVE	681.0	603.0	489.0	510.0	534.0
NARCliM	**AUE**	**SES**	**SEE**	**SEN**	**Av S, E, N**
NARCliM-K-ACESS1-0	646	563	364	410	445.7
NARCliM-K-CanESM2	670	500	454	486	480.0
NARCliM-K-ACCESS1-3	600	576	374	356	435.3
NARCliM-J-ACCESS1-0	682	549	333	476	452.7
	AUE	**SES**	**SEE**	**SEN**	**Av S, E, N**
BARPA-ACCESS1-0	746	698	596	579	624.4

Table 7. Skill score M averaged over the three variables air temperature, precipitation and sea-level pressure. Values are given for the four regions and each model. Top table, CMIP5, 2nd table for CCAM from the 12km grid, 3rd table as NARCliM 50km and 4th table is for BARPA. Also given is the average over six model results in each case, and the average of the S, E and N results (at right). The models are ACCESS1-0, GFDL-ESM2M, CNRM-CM5, CanESM2, NorESM1-M, and MIROC5. Regions are shown in Figure 17.

The improvement of CCAM, over CMIP5, is evidently due to the simulation of detail in the precipitation fields. It indicates an 'added value' of CCAM. CCAM does produce on average higher rainfall and lower temperatures than the driver models. However, the reduced rainfall for the ERA5 case (not shown) suggests that tuning a downscaling model to produce a more realistic mean rainfall is not a simple process. The NARCliM-K M scores are lower for 6 of the 8 common cases. This may be partly due to the lower resolution of NARCliM, and hence smaller spatial variation, especially in the smaller regions. NARCLiM-J gives slightly better scores for ACCESS1-0. BARPA is better again, providing considerable 'added value'.

Further assessment is warranted, but from these results all the ESCI datasets considered here appear credible as representations of the basic climate from the recent past. Nevertheless, the relative coolness of the CCAM simulations for the recent past suggests that using the QME version of the air temperature values, in particular, may be worthwhile, for some applications.

4.5 Projected change: representing the range of possibilities from CMIP5 models

Another consideration when evaluating downscaling of GCMs with RCMs is how well the downscaled change in climate represents the full range of possibilities simulated by the different CMIP5 GCMs (this is also quantified by PAV discussed in the next section). For this comparison we will sample a few downscaled GCMs for different methods and compare the change in climate for 2040-2059 relative to 1986-2005 under the RCP8.5 emission pathway.

Figure 18 shows the results for BARPA after downscaling ACCESS1-0. In general, the change in both daily maximum and daily minimum temperature is reasonably similar to that projected by the host GCM. We note that in this case BARPA and ACCESS1-0 share a common land-surface model, atmospheric physics and other components. Nevertheless, we are confident that BARPA is performing well at representing the changes projected by ACCESS, but with enhanced regional features. This is particularly noticeable where the change in projected rainfall for 2040-2059 relative to 1986-2005 (RCP8.5) clearly shows changes due to the improved resolution, such as enhancements for coastal regions and areas of complex topography like the Australian alps. Nevertheless, the broad changes in rainfall are still somewhat consistent with the host GCM.

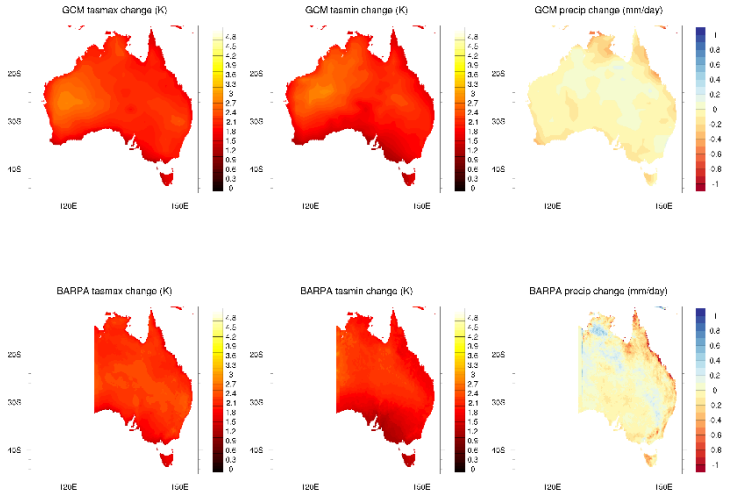

Figure 18: BARPA daily maximum temperature change (left column), daily minimum temperature change (middle column) and precipitation change (right column) for 2040-2059 relative to 1986-2005 for the RCP8.5 emission pathway. Top row is GCM change and bottom row is BARPA change. One GCM is considered being ACCESS1-0.

Figures 19 to 21 show a comparison of the projected change in daily maximum air temperature, daily minimum air temperature and precipitation for NARCliM v1.5 for 2040-2059 relative to 1986-2005 under the RCP8.5 emission pathway. In this comparison there are the GCM (top row), NARCliM J configuration (middle row) and NARCliM K configuration (bottom row). The three GCMs considered are ACCESS1-0 (left column), ACCESS1-3 (middle column) and CanESM2 (right column). We note that the NARCliM v1.5 results shown here are from the 50km resolution CORDEX Australasia domain. The results indicate that the choice of NARCliM v1.5 configuration can impact on the change signal. For example, the NARClIM J configuration somewhat resembles the amount of warming shown in the host GCM, whereas NARCliM K configuration shows more warming after downscaling ACCESS1-0 than when downscaling CanESM2 for Western Australia. Dynamical downscaling techniques can alter the projected change in climate as they have their own representation of atmosphere physical processes and dynamical behaviour. In some cases, the RCMs add value through their ability to respond to local topographical features or improved resolution of atmospheric processes.

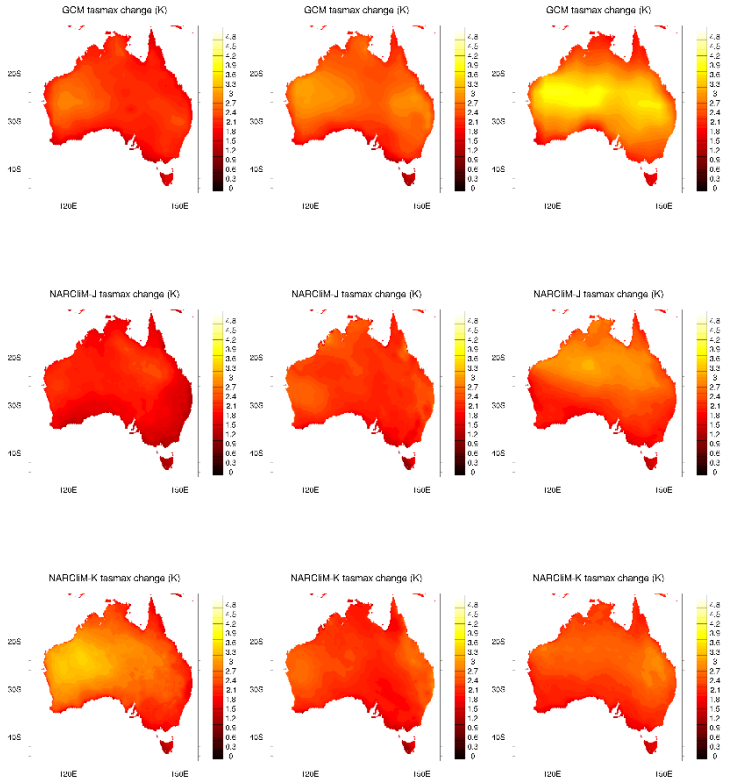

Figure 19: NARCliM v1.5 daily maximum temperature change for 2040-2059 relative to 1986-2005 for the RCP8.5 emission pathway. Top row is GCM change, the middle row is the NARCliM-J change and bottom row is NARCliM-K change. Three GCMs are considered being ACCESS1-0 (1st column), ACCESS1-3 (2nd column) and CanESM2 (3rd column).

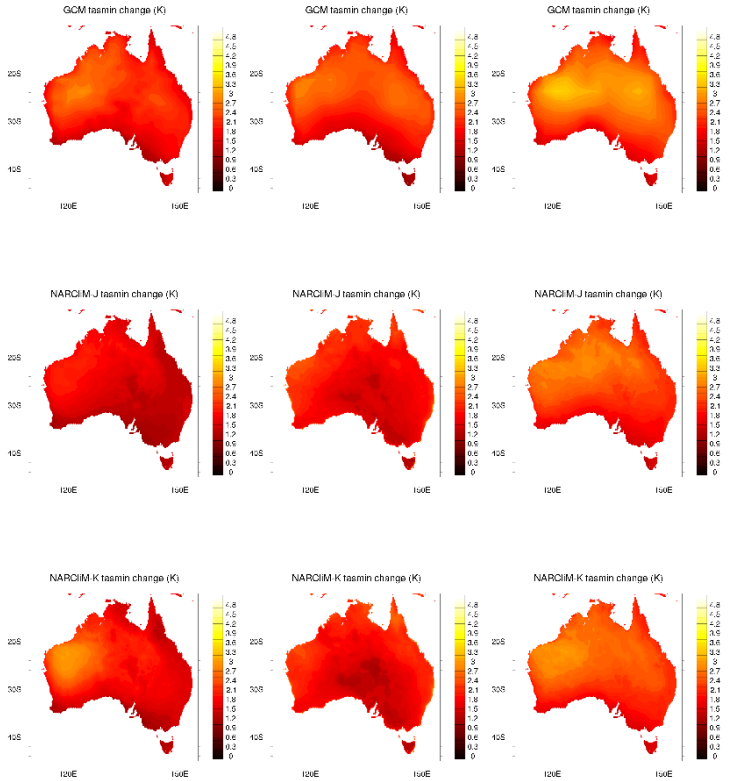

Figure 20: NARCliM v1.5 daily minimum temperature change for 2040-2059 relative to 1986-2005 for the RCP8.5 emission pathway. Top row is GCM change, the middle row is the NARCliM-J change and bottom row is NARCliM-K change. Three GCMs are considered being ACCESS1-0 (1st column), ACCESS1-3 (2nd column) and CanESM2 (3rd column).

The projected change in precipitation from NARCliM v1.5 is shown in Figure 19, relative to the host GCMs. For ACCESS1-3 (middle column) and CanESM2 (right column) the changes in precipitation are comparable to the host GCMs, although with some regional differences. In the case of NARCliM downscaling ACCESS1-0 (left column), there is a tendency to show an increased amount of drying for the eastern side of Australia.

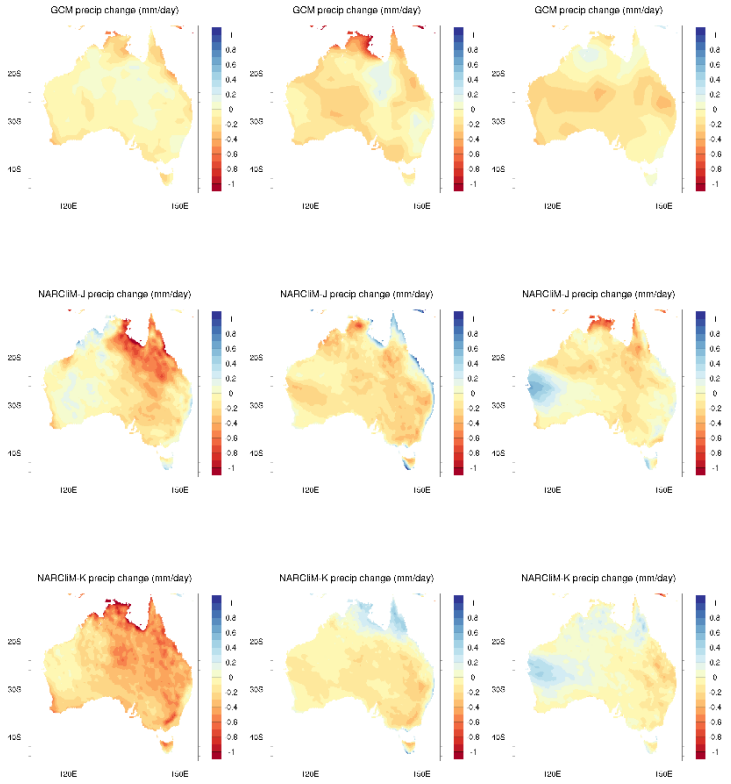

Figure 21: NARCliM v1.5 daily precipitation change for 2040-2059 relative to 1986-2005 for the RCP8.5 emission pathway. Top row is GCM change, the middle row is the NARCliM-J change and bottom row is NARCliM-K change. Three GCMs are considered being ACCESS1-0 (1st column), ACCESS1-3 (2nd column) and CanESM2 (3rd column).

Figures 22 to 24 show the projected changes from the CCAM downscaling for 2040-2059 relative to 1986-2005 under the RCP8.5 emission pathway. We have plotted five examples of CCAM downscaled GCMs, with CCAM-NorESM1-M as a medium case model (1st column), CCAM-MIROC5 as a low warming model (2nd column), CCAM-ACCESS1-0 as a medium warming model (3rd column), then with CCAM-GFDL-ESM2M as a higher warming model (4th column) and CCAM-CanESM2 as a high warming model (5th column). For the daily maximum temperature, CCAM can be seen to produce a change signal that is relatively similar to the host GCM, although the amount of warming is slightly lower than that projected by the host GCM. However, in the case of daily minimum temperatures in Figure 23, we notice that three out of the four downscaled GCMs in this figure show a consistent increase in minimum temperature with the host GCM, with CCAM-GFDL-ESM2M showing an alternative result where the minimum temperature changes by a much smaller amount. Since we have two examples of high warming with CCAM-GFDL-ESM2M and CCAM-CanESM2, we note that the reduced amount of warming for the minimum temperature is somewhat specific to GFDL-ESM2M and is not the case in general as shown by CCAM-CanESM2 with a much higher increase in daily minimum temperature. This difference in CCAM-GFDL-ESM2M from the host GCM is likely to be related to changes in cloud cover and is currently being investigated.

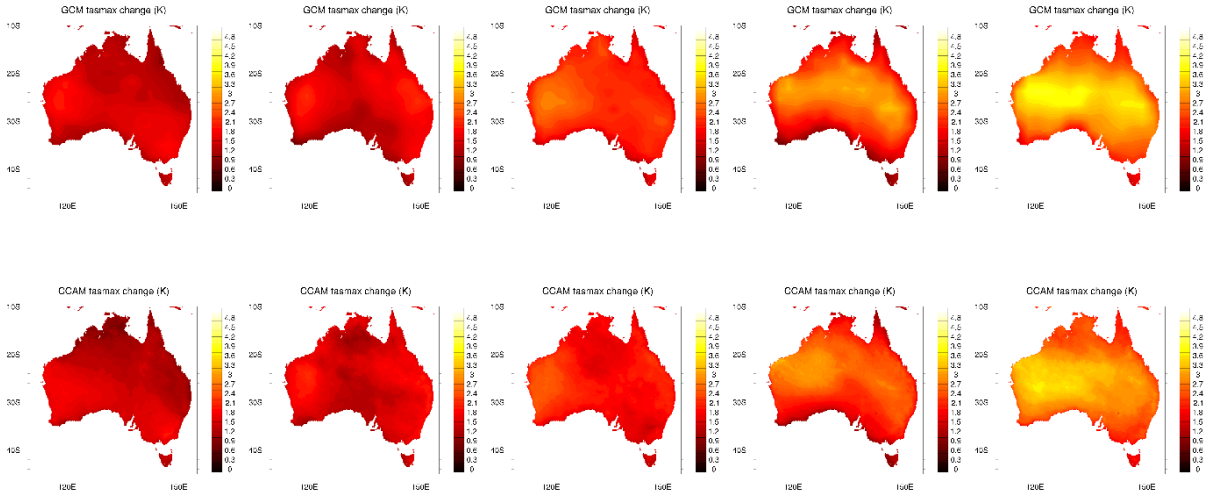

Figure 22: CCAM daily maximum temperature change for 2040-2059 relative to 1986-2005 for the RCP8.5 emission pathway. Top row is GCM change and bottom row is CCAM change. Five GCMs are considered being NorESM1-M (1st column), MIROC5 (2nd column) and ACCESS1-0 (3rd column), GFDL-ESM2M (4th column) and CanESM2M (5th column).

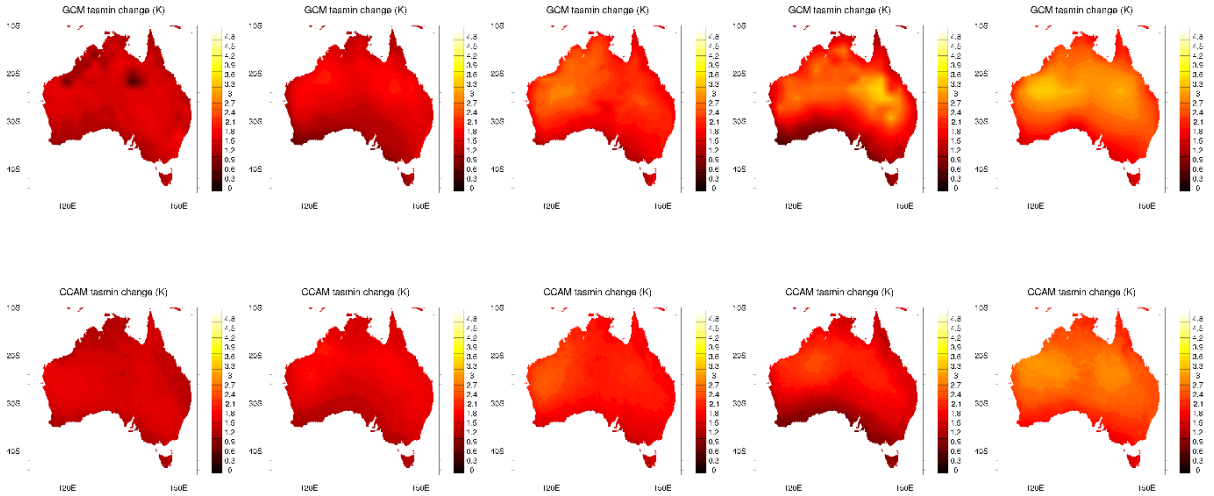

Figure 23: CCAM daily minimum temperature change for 2040-2059 relative to 1986-2005 for the RCP8.5 emission pathway. Top row is GCM change and bottom row is CCAM change. Five GCMs are considered being NorESM1-M (1st column), MIROC5 (2nd column) and ACCESS1-0 (3rd column), GFDL-ESM2M (4th column) and CanESM2 (5th column).

In Figure 24 we compare the changes in precipitation between the GCMs and the CCAM downscaled simulations. As was the case for BARPA, we notice a number of local enhancements to the change in rainfall, particularly along coastlines and for areas of complex topography such as the Australian alps. Also, like BARPA, CCAM is broadly consistent with the host GCM despite using a single cloud microphysics parameterisation compared to each GCM using a different parameterisation for clouds. We are therefore confident that CCAM is generally consistent with the host GCM, although it can change the projection as was demonstrated for the GFDL-ESM2M GCM.

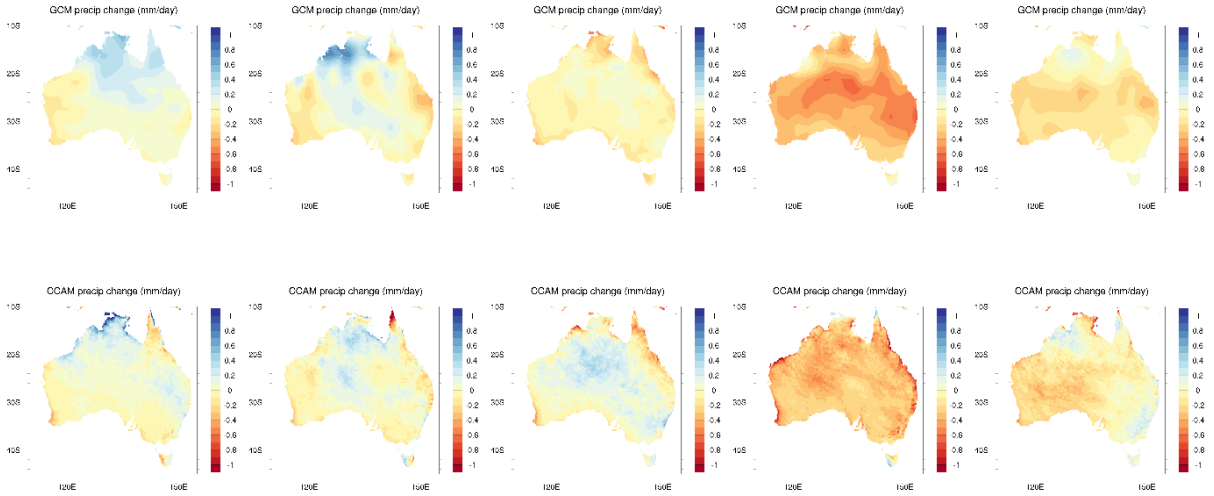

Figure 24: CCAM precipitation change for 2040-2059 relative to 1986-2005 for the RCP8.5 emission pathway. Top row is GCM change and bottom row is CCAM change. Five GCMs are considered being NorESM1-M (1st column), MIROC5 (2nd column) and ACCESS1-0 (3rd column), GFDL-ESM2M (4th column) and CanESM2 (5th column).

4.6 Projected changes: Realised added value

A tool for quantifying the benefit of performing downscaling is realised added value (RAV) (Di Virgilio et al 2020). This analysis is based on three quantities, known as added value (AV), potential added value (PAV) and finally realised added value (RAV). AV describes how an RCM improves on its host model's simulated climate for a historical period when compared to observations (i.e., higher AV is better). PAV quantifies how an RCM modifies the projected changes with respect to the host model. PAV of zero indicates that the RCM projects the same future change as the GCM, while a non-zero PAV indicates that the RCM projected change differs from the GCM projected change in the direction indicated. Finally, AV and PAV are used to show RAV as an overall summary of the value added by the RCM. Hence, high (positive) RAV indicates that the RCM improves the historical simulation (positive AV) and that the RCM projection differs from the GCM projection (PAV is non-zero). Negative regions of AV, PAV and RAV are possible (blue regions in Figures 25 to 30). For example, negative AV tends to indicate that the host GCM was already very similar to gridded observation data. Note that a negative PAV can also be a positive contribution to RAV, but differ in terms of the sign or size of the projected change.

Below in Figures 25 to 30, we show the basic RAV for the three dynamical downscaling models used in ESCI being BARPA, NARCliM and CCAM with respect to temperature and precipitation means as well as extremes. In all cases, downscaling of ACCESS1-0 was used as it was the GCM that was downscaled by all three models. Starting with daily maximum 2m air temperature and extreme daily maximum temperature (represented by the 99th percentile over a 20-year period) for 1986-2005 shown in Figures 25 and 28, we note that the downscaling has a mix of locations for both positive and negative RAV. In the left column we can see some regions which clearly contribute to positive AV with respect to historical observations relative to the host GCM, as well as regions which perform less well reflecting the widespread cold bias shown in Figure 4. The extreme 99th percentile for daily maximum temperature tends to show the dynamically downscaling RCMs having more positive AV than the average daily maximum temperature, suggesting RCM results may be more useful for extreme temperatures than the average temperature. The middle column indicates whether the RCM provided a

different change in the future regional climate for 2080-2099 relative to 1986-2005. We note that BARPA in particular provides a high positive PAV, projecting higher temperature increases than the driving GCM. NARCliM-J and CCAM tend to project lower temperature increases than the driving GCM for most regions. The AV and PAV are then combined into RAV on the right column. There is a tendency for the RCMs to add positive RAV along coastal and tropical regions being areas that GCMs find difficult to adequately resolve. There is a tendency to show positive RAV from downscaling for the extreme maximum temperature, although this can vary between different downscaling models. Nevertheless, the results illustrate some of the advantages of using a multi-model approach.

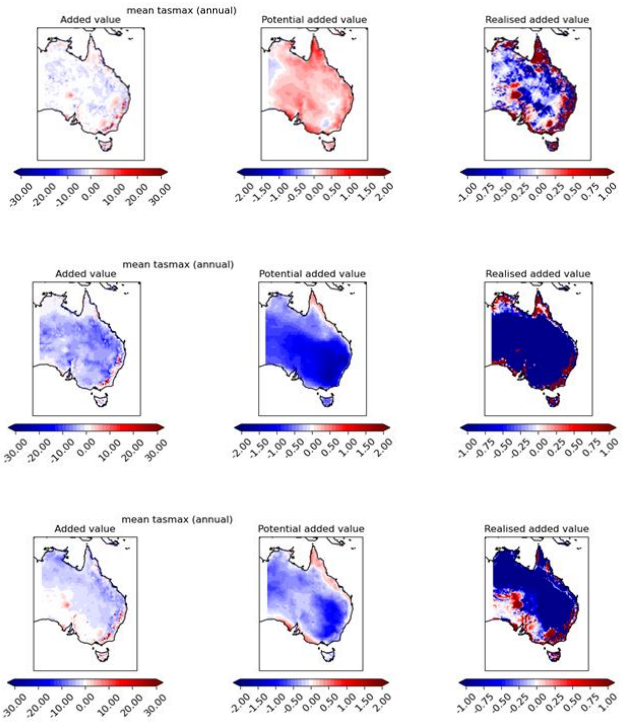

Figure 25: Plots of the added value (left column), potential added value (middle column) and realized added value (right column) for BARPA (top row), NARCliM-J (middle row) and CCAM (bottom row) with respect to average daily maximum 2m air temperature after downscaling ACCESS1-0 for 2080-2099 relative to 1986-2005.

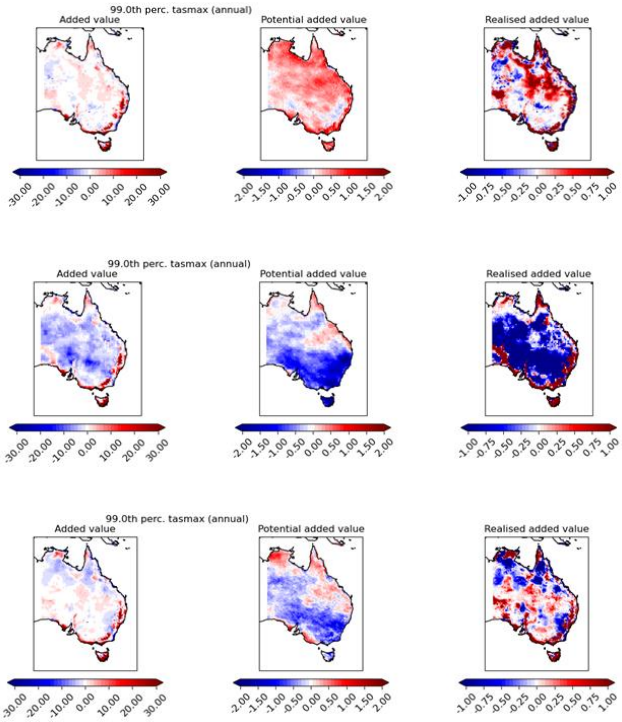

Figure 26: Same as for figure 24, but for the 99th percentile of daily maximum temperature as an indication of an extreme daily maximum temperature after downscaling ACCESS1-0 for 2080-2099 relative to 1986-2005. Columns denote added value (left), potential added value (middle) and realized added value (right). Rows show BARPA (top), NARCliM-J (middle) and CCAM (bottom).

In the case of minimum daily 2m air temperature (figures 27 and 28) we note that on average the RCMs do a better job of increased realised added value to the mean daily minimum temperature compared to the maximum temperature described in figures 26 and 26. There is also a much larger area where the RCMs add value with the downscaling of extreme minimum temperatures compared to extreme daily maximum temperatures.

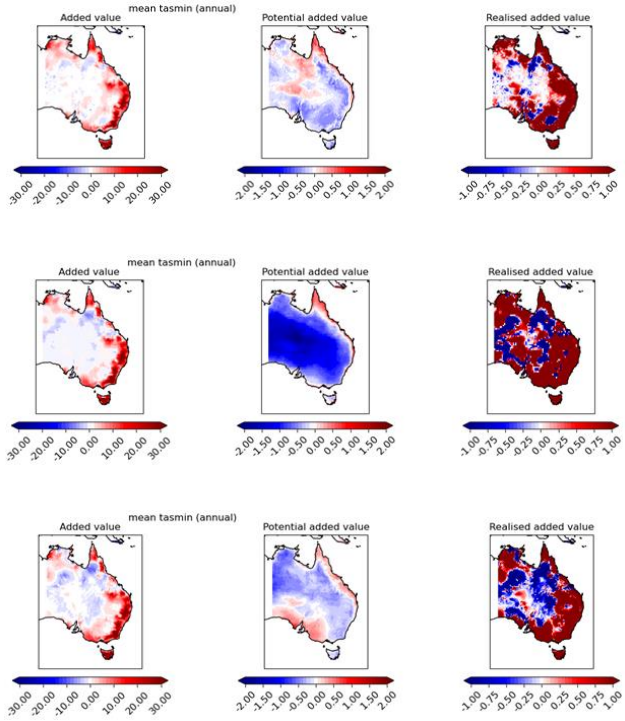

Figure 27: Same as figure 25, but for average daily minimum temperature after downscaling ACCESS1-0 for 2080-2099 relative to 1986-2005. Columns denote added value (left), potential added value (middle) and realized added value (right). Rows show BARPA (top), NARCiM-J (middle) and CCAM (bottom).

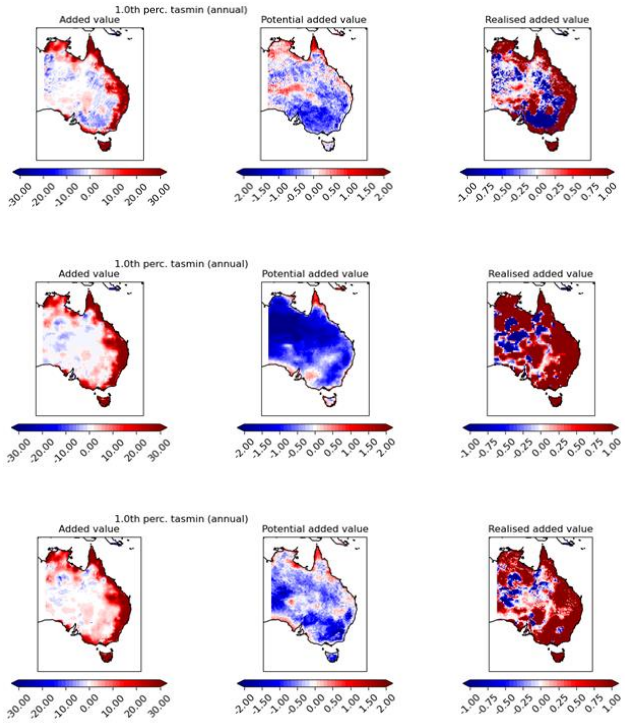

Figure 28: Same as figure 25, but for 1st percentile daily minimum temperature as a representation of extreme cold temperatures after downscaling ACCESS1-0 for 2080-2099 relative to 1986-2005. Columns denote added value (left), potential added value (middle) and realized added value (right). Rows show BARPA (top), NARCliM-J (middle) and CCAM (bottom).

Finally, in Figures 29 and 30 we consider added value for precipitation. The RAV for mean rainfall is somewhat varied between the downscaled models, although certainly with examples of clear positive RAV. Again, the RAV for the extreme daily precipitation appears to be more positive than for the average precipitation, once more suggesting that the downscaling is adding more value for the extreme weather than for the average weather. There is also a tendency to improve precipitation in the tropics, coastal regions and regions of complex topography.

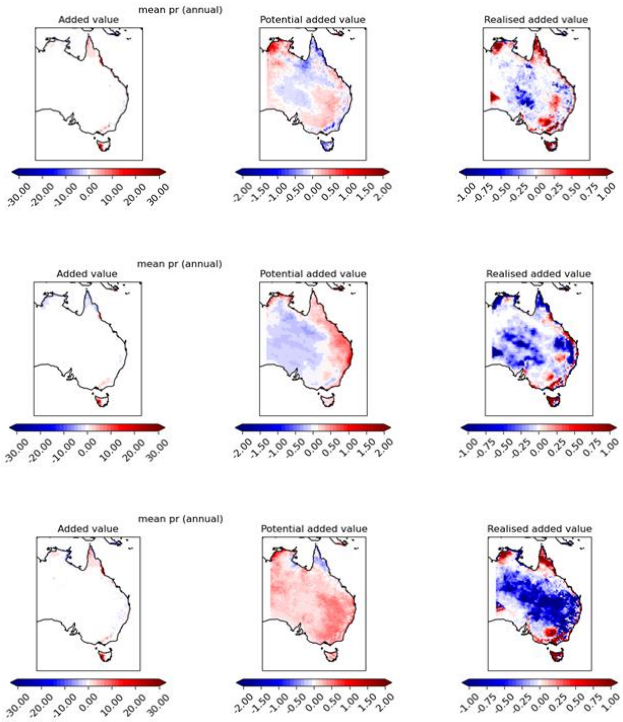

Figure 29: Same as figure 25, but for average daily precipitation after downscaling ACCESS1-0 for 2080-2099 relative to 1986-2005. Columns denote added value (left), potential added value (middle) and realized added value (right). Rows show BARPA (top), NARCiM-J (middle) and CCAM (bottom).

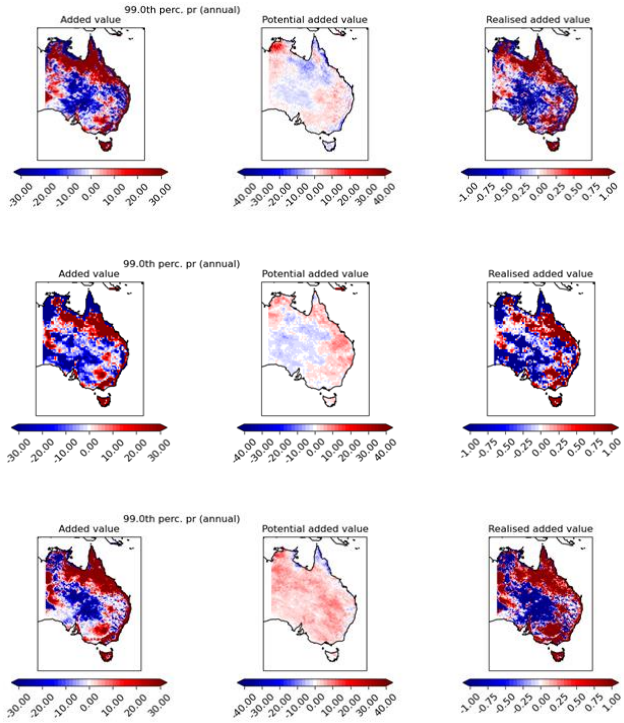

Figure 30: Same as figure 25, but for 99th percentile of daily precipitation as a representation of extreme rainfall after downscaling ACCESS1-0 for 2080-2099 relative to 1986-2005. Columns denote added value (left), potential added value (middle) and realized added value (right). Rows show BARPA (top), NARCliM-J (middle) and CCAM (bottom).

A useful summary of the RAV is shown in figure 31 between BARPA, NARCliM-J and CCAM with respect to correlation. From this figure it is clear that generally regions of complex topography have more RAV due to downscaling, coastal regions in the middle and flat regions with the least RAV. The situation can be different when focusing on extreme temperatures and rainfall which improve over larger areas. Importantly the best performance for different seasons and different levels of extremes can vary between RCMs, thereby demonstrating the value of a multi-model approach.

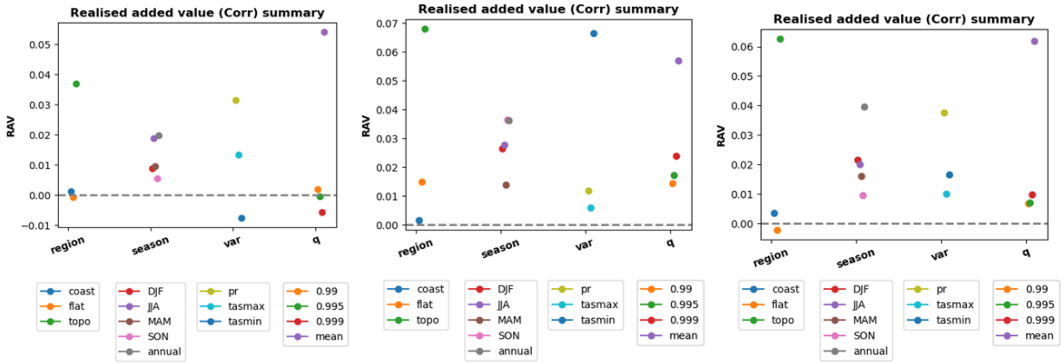

Figure 31: Summary of realized added value for temperature and precipitation in terms of correlation with observations after downscaling from ACCESS1-0. The plots represent BARPA (left), NARCiM-J (middle) and CCAM (right).

It is important to note that applying QME to the downscaling results can significantly improve their RAV. PAV for the RCMs with QME calibration applied can be compared to PAV for the GCMs with QME applied, with QME improving AV in both cases (due to its quantile matching basis), but showing improvements in PAV for the RCM calibrated data over the GCM calibrated data. Examples are shown in figures 32 to 34, which describe AV, PAV and RAV after QME calibration has been applied to the ACCESS1-0 GCM as well as the regional models for average daily maximum, average daily minimum and average daily rainfall, respectively. After QME calibration has been applied, the added value is considerably more positive across Australia. Note that more value is added when using RCM-QME than the GCM-QME applied for ACCESS1-0, due to the improvement in PAV. Essentially the PAV for the ACCESS1-0 GCM is close to zero, whereas the PAV for the regional models is strongly non-zero for the regional models (indicating a difference in the projected change).

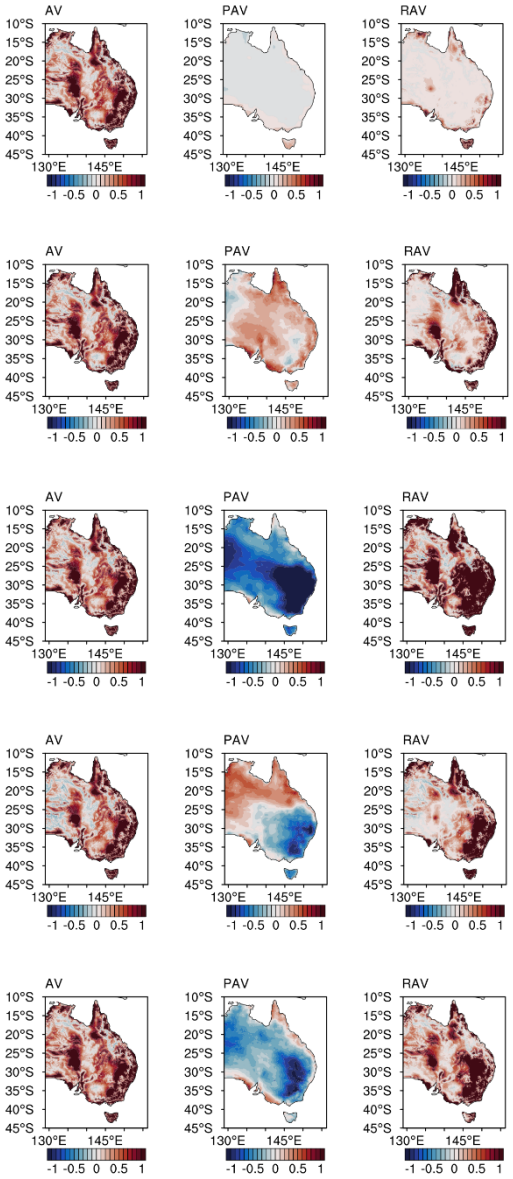

Figure 32: Realized added value for daily maximum temperatures after QME calibration is applied to GCMs and RCMs for ACCESS1-0. Left column is added value, middle column shows potential added value and the right column shows realized added value. Top row is for ACCESS1-0 GCM, 2nd row is for BARPA-ACCESS1-0, 3rd row shows NARCliM-J-ACCESS1-0, 4th row shows NARCliM-K-ACCESS1-0 and 5th row shows CCAM-ACCESS1-0. All results are for 2080-2099 with respect to 1986-2005 and under the RCP8.5 emission scenario.

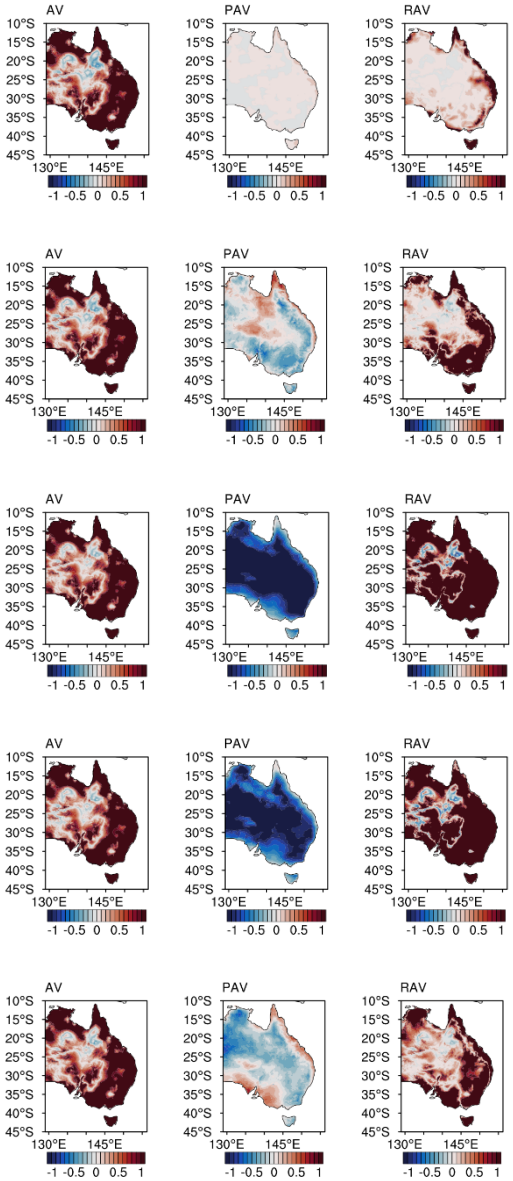

Figure 33: Realized added value for daily minimum temperatures after QME calibration is applied to GCMs and RCMs for ACCESS1-0. Left column is added value, middle column shows potential added value and the right column shows realized added value. Top row is for ACCESS1-0 GCM, 2nd row is for BARPA-ACCESS1-0, 3rd row shows NARCliM-J-ACCESS1-0, 4th row shows NARCliM-K-ACCESS1-0 and 5th row shows CCAM-ACCESS1-0. All results are for 2080-2099 with respect to 1986-2005 and under the RCP8.5 emission scenario.

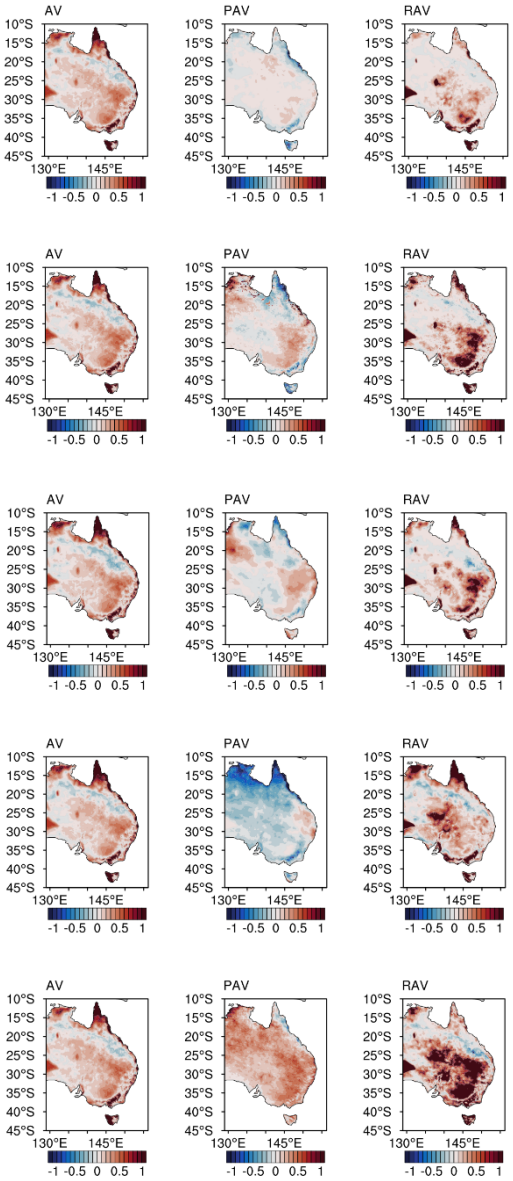

Figure 34: Realized added value for daily rainfall after QME calibration is applied to GCMs and RCMs for ACCESS1-0. Left column is added value, middle column shows potential added value and the right column shows realized added value. Top row is for ACCESS1-0 GCM, 2nd row is for BARPA-ACCESS1-0, 3rd row shows NARCliM-J-ACCESS1-0, 4th row shows NARCliM-K-ACCESS1-0 and 5th row shows CCAM-ACCESS1-0. All results are for 2080-2099 with respect to 1986-2005 and under the RCP8.5 emission scenario.

5. Conclusions

This report describes the downscaling of global climate projections to regional scales for the purposes of ESCI and stakeholders in the electricity sector. These climate datasets are intended to assist with stakeholders quantifying climate-related risks posed by global warming. Although we intend for these datasets to be useful for a broad range of users, we note that they can be considered to support

existing climate datasets that may have already been in use in the sector (e.g., data from Climate Change in Australia). The use of these downscaled datasets provides additional information and scenarios that could be used for a range of risk assessments.

Although this document is intended as a technical reference for the various downscaled datasets, we note that the science is continually improving as we gather further lines of evidence. Hence the results of this work will continue to be updated into the future. For example, BARPA was intended for ESCI to cover eastern Australia using RCP8.5, and building on the successful delivery of that a new project is currently running BARPA for western Australia and RCP4.5 to enable national coverage for two emissions pathways (contact Bureau of Meteorology for further details as required). The information in this report is designed to help with understanding some of the advantages and disadvantages of different downscaling techniques, noting that there is no case where one method consistently provides superior results compared to the other methods. Therefore, it is generally recommended to consider a broad range of model data and other lines of evidence (e.g., observations data can provide insight on extremes and climate change trends). Further details on lines of evidence for extremes are available in the SMPL Technical Report, as well as details on model choice and recommendations in the range of less technical guidance material produced by the ESCI project for more practical energy sector applications.

Tools such as Realised Added Value (RAV) can be useful for comparing the techniques including assessment of biases in relation to observations for the historical period, as well as how downscaling can modify the future projections from coarser-scale GCM output.

The report also provides an analysis of extreme events based on average recurrence interval, as well as some derived datasets that represent various hazards (e.g., including bushfire weather conditions). These hazard datasets can be either used directly by the stakeholders or as a secondary check on independent hazard modelling.

RCMs do not automatically fix all problems with climate simulations. Calibration methods are generally recommended to be applied to RCM (and to GCM) projections in this project. For example, NARCLiM and CCAM show a cold bias in their simulations, which the calibrated method then accounts for. This also helps the data to be more readily applicable in user applications. RCMs also show some extremes that are too wet in parts of northern Australia and along coastlines (noting that AWAP may be underestimating extremes in some regions). Nevertheless, RCMs generally improve on the GCMs which struggle to represent the extreme rainfall. Realised Added Value is not uniformly positive when simply downscaling. However, when combining downscaling with bias correction like QME, we find a general improvement in the simulated climate.

The computing resources required for downscaling constrain the ensemble size to be somewhat smaller than is the case for GCMs. This is also a reflection that an individual country does not have the same resources as a multi-nation intercomparison experiment. In this way the regional climate simulations will not perfectly represent the full range of the CMIP5 ensemble of climate simulations. Nevertheless, effort was made to downscale GCMs recommended by CCiA so as to have the best chance of representing low, mid and high changes in temperatures and rainfall. Since regional models have their own physical parameterisations, they can disagree with the host global climate model, particularly with respect to changes in rainfall (a highly complex and non-linear process dependent on many physical drivers over a range of spatio-temporal scales). We also note that when global climate models are simulated at different resolutions, the same model can also produce different projections for rainfall and temperature, so it is not entirely unexpected that regional models respond differently to the

host GCMs. It is also a complex task to break down the reasons for different projections without running a number of new downscaling experiments designed to isolate the impact of various factors (e.g., turning on or off aerosols, or running different physical parameterisations as was done for NARCliM).

The work represented in this report is one of the larger regional downscaling intercomparisons undertaken for Australia, along with the CORDEX Australasia intercomparison experiment. Combined with the GCM projections already undertaken as part of Climate Change in Australia, and the standardised method for projections likelihood (SMPL) these datasets can assist the electricity sector in assessing and adapting to climate-related risks now and into the future years.

6. References

Brown, A. and Dowdy, A., 2021. Severe convection-related winds in Australia and their associated environments. Journal of Southern Hemisphere Earth Systems Science, 71(1), pp.30-52.

Christensen, J.H., Carter, T.R., Rummukainen, M., Amanatidis, G., 2007. Evaluating the performance and utility of regional climate models: the PRUDENCE project. *Climatic Change* 81, 1–6, doi.org/10.1007/s10584-006-9211-6

CSIRO and Bureau of Meteorology 2015, Climate Change in Australia Information for Australia's Natural Resource Management Regions: Technical Report, Climate Change in Australia, accessed online:
https://climatechangeinaustralia.gov.au/media/ccia/2.2/cms_page_media/168/CCIA_2015_NRM_TechnicalReport_WEB.pdf.

Di Virgilio, G., Evans, J., Di Luca, A., Grose, M., Round, V. and Thatcher, M. J., 2020, Realised added value in dynamical downscaling of Australian climate change, Clim. Dyn., 54, 4675–4692, doi.org/10.1007/s00382-020-05250-1

Dowdy, A. J., Grose M. R., Timbal B., Moise A., Ekstrom M., Bhend J. and Wilson L., 2015. Rainfall in Australia's eastern seaboard: a review of confidence in projections based on observations and physical processes. *Aust. Met. Oceanog. J.* 65, 107-126

Dowdy, A.J., Ye, H., Pepler, A., Thatcher, M., Osbrough, S.L., Evans, J.P., Di Virgilio, G. and McCarthy, N., 2019. Future changes in extreme weather and pyroconvection risk factors for Australian wildfires. *Scientific reports*, *9*(1), pp.1-11.

Dowdy, A. J., 2019. Towards seamless predictions across scales for fire weather, accessed online:
http://albuquerque.firebehaviorandfuelsconference.com/wpcontent/uploads/sites/13/2019/04/Dowdy-Sydney.pdf

Dowdy, A.J., 2020. Seamless climate change projections and seasonal predictions for bushfires in Australia. *Journal of Southern Hemisphere Earth Systems Science*, *70*(1), 120-138, doi.org/10.1071/ES20001.

Evans J. P., Ji, F., Lee, C., Smith, P., Argüeso, D., Fita, L., 2014. Design of a regional climate modelling projection ensemble experiment – NARCliM. *Geosci Model Dev* 7:621–629.

Evans, J. P., Di Virgilio, G., Hirsch, A. L., Hoffmann, P., Remedio, A. R., Ji, F., Rockel, B., Coppola, E., 2021. The CORDEX-Australasia ensemble: evaluation and future projections. *Clim. Dyn.*, doi.org/10.1007/s00382-020-05459-0

Giorgi, F., Gutowski, W. J., 2016. Coordinated Experiments for Projections of Regional Climate Change. Curr Clim Change Rep 2, 202–210 doi.org/10.1007/s40641-016-0046-6

Kidson, J. W., 1988. Indices of the Southern Hemisphere Zonal Wind, *J. Climate*, 1, 183-194, doi.org/10.1175/1520-0442(1988)001%3C0183:IOTSHZ%3E2.0.CO;2

King, A. D., Alexander, L. V. and Donat, M. G., 2013. The efficacy of using gridded data to examine extreme rainfall characteristics: a case study for Australia. Int. J. Climatol. 33. 2376-2387. doi.org/10.1002/joc.3588

McArthur, A. G., (1967.) Fire Behaviour in Eucalypt Forests. Department of National Development Forestry and Timber Bureau, Canberra, Leaflet 107.

McGregor, J. L., 2005. C-CAM: Geometric aspects and dynamical formulation. CSIRO Marine and Atmospheric Research Tech. Paper 70, 43 pp

Murray, R. J., and I. Simmonds, 1991: A numerical scheme for tracking cyclone centres from digital data Part I: development and operation of the scheme. Aust. Met. Mag. 39, 155–166. **https://www.metoffice.gov.uk/pub/data/weather/uk/ukcp18/science-reports/UKCP18-Land-report.pdf**.

Murphy J. M., Harris, G. R., Sexton, D. M. H., Kendon, E. J., Bett, P. E., Clark, R. T., Eagle, K. E., Fosser, G., Fung, F., Lowe, J. A., McDonald, R. E., McInnes, R. N., McSweeney, C. F., Mitchell, J. F. B., Rostron, J. W., Thornton, H. E., Tucker, S., Yamazaki, K., 2018. UKCP18 land projections: Science report, accessed online: **https://www.metoffice.gov.uk/pub/data/weather/uk/ukcp18/science-reports/UKCP18-Land-report.pdf**.

Pepler, A. S., Di Luca, A., Ji, F., Alexander, L. V., Evans, J. P., Sherwood, S. C., 2015. Impact of identification method on the inferred characteristics and Variability of Australian East Coast Lows. Mon. Wea. Rev. 143. 864-876. doi.org/10.1175/MWR-D-14-00188.1

Simmonds, I., and R. J. Murray, 1999: Southern extratropical cyclone behavior in ECMWF analyses during the FROST Special Observing Periods. *Wea. Forecasting*, 14, 878–891.

Stevens, B., Fiedler, S., Kinne, S., Peters, K., Rast, S., Müsse, J., Smith, S. J., Mauritsen, T., 2017. MACv2-SP: a parameterization of anthropogenic aerosol optical properties and an associated Twomey effect for use in CMIP6, *Geosci. Model Dev.*, 10, 433–452, doi:10.5194/gmd-10-433-2017.

Su, C.-H., Eizenberg, N., Steinle, P., Jakob, D., Fox-Hughes, P., White, C. J., Rennie, S., Franklin, C., Dharssi, I., Zhu, H., 2019, BARRA v1.0: the Bureau of Meteorology Atmospheric high-resolution Regional Reanalysis for Australia, *Geosci. Model Dev.*, 12, 2049–2068, doi:10.5194/gmd-12-2049-2019.

Su, C.-H., Eizenberg, N., Jakob, D., Fox-Hughes, P., Steinle, P., White, C. J., and Franklin, C., 2020. BARRA v1.0: Kilometre-scale downscaling of an Australian regional atmospheric reanalysis over four midlatitude domains, *Geosci. Model Dev. Discuss.*, doi:10.5194/gmd-2020-366, in review.

Su, C.-H., Ye, H., Dowdy, A., Pepler, A., Stassen, C., Brown. A., Tucker, S. O., Steinle, P. J., 2021. Towards ACCESS-based regional climate projections for Australia, Submitted to *Geosci. Model Dev.*

Thatcher, M. J. and McGregor, J. L., 2009. Using a scale-selective filter for dynamical downscaling with the conformal cubic atmospheric model. *Mon. Wea. Rev.*, 137, 1742–1752

Watterson, I. G., 2009. Components of rainfall and temperature anomalies and change associated with modes of the Southern Hemisphere, *Int. J. Climatol.*, 29, 809-826, DOI: 10.1002/joc.1772

Watterson, I.G., 2015 Improved simulation of regional climate by global models with higher resolution: skill scores correlated with grid length. *J. Climate*, 28, 5985-6000.

Watterson, I. G., 2019a. Indices of climate change based on patterns from CMIP5 models, and the range of projections. *Climate Dynamics*, 52, 2451-2466, doi 10.1007/s00382-018-4260-x

Watterson, I. G., 2019b. Influence of sea surface temperature on simulated future change in extreme rainfall in the Asia-Pacific. On-line, *Asia-Pacific J. Atmos. Sci.* doi 10.1007/s13143-019-00141-w

Watterson, I. G., 2020. Australian Rainfall Anomalies in 2018-2019 Linked to Indo-Pacific Driver Indices using ERA5 Reanalyses. J. Geophysical Res, 125. Doi 10.1029/2020JD033041


ELECTRICITY
SECTOR
CLIMATE
INFORMATION
PROJECT